

QUANTIFICATION OF THE CEPHALOPOD
SUTURE PATTERN

By

Douglas John Canfield

A THESIS

Submitted to

Michigan State University

in partial fulfillment of the requirements

for the degree of

MASTER OF SCIENCE

Department of Geology

1977

THE UNIVERSITY OF CHICAGO
LIBRARY

1967

1967

1967

1967

1967

1967

1967

1967

1967

ABSTRACT

QUANTIFICATION OF THE CEPHALOPOD SUTURE PATTERN

By

Douglas John Canfield

The Fourier series exactly describes the shape of cephalopod suture patterns in the subclasses Nautiloidea, Bac-tritoidea, and in four of the eight orders of the Ammonoidea, but can not presently describe complex ammonitoid sutures. The Fourier method allows the calculation and graphical display of the mean sutural patterns of the subclasses and orders studied, and exactly quantifies the morphological differences between groups. Discriminant analysis provides significant differentiation of the four ammonoid orders using only the Fourier harmonic amplitudes of the sutures. Discriminant analysis also reveals significant and otherwise undetectable differences between the two symmetric halves of sutures in Acanthoclymenia neapolitana, and thereby measures the non-genetic norm of reversion in that species. Specific harmonic amplitudes increase monotonically in the ontogeny of Koenenites cooperi as well as in the phylogeny of four genera of the family Gephuroceratidae, with the result that the ontogenetic and phylogenetic scaling factors are statistically identical, confirming on a quantitative basis the assumption of recapitulatory evolution in this lineage.

TABLE OF CONTENTS

	Page
Acknowledgments	i
List of Tables.	ii
List of Figures	iv
Introduction.	1
Methods	4
Results	13
Summary and Conclusions	44
List of References.	46
Appendix A	48
B	51
C	52
D	57
E	61
F	64

ACKNOWLEDGEMENTS

I wish to thank Dr. Robert L. Anstey for his advice and guidance throughout this project. The helpful criticisms of Dr. Duncan Sibley and Dr. John Wilband are also greatly appreciated. Special thanks are given to Mitch Roth and Lloyd Lerew for their assistance with understanding mathematical, computational and philosophical problems.

LIST OF TABLES

	PAGE
TABLE 1: Values of the Coefficient of Variation (CV) for six replications of <u>Koenenites cooperi</u> and seven replications of <u>Goniatites choctawensis</u>	14
TABLE 2: Mean values for the Coefficient of Variability computed for the taxonomic hierarchy.	15
TABLE 3: Summary of Discriminant Analysis of data from sutures in the Orders Anarcestinda, Clymeniida, Goniatitida, and Ceratitida.	23
TABLE 4: Summary of Discriminate Analysis of data from <u>Acanthoclymenia neapolitana</u> . Perfect discrimination between left and right suture halves in both juvenile and adult sutures demonstrates presence of nongenetic influences on suture shape.	24
TABLE 5: Rankings of the harmonic amplitudes within each harmonic frequency for six suture patterns in the ontogenetic series of <u>Koenenites cooperi</u> . The increase in rank sums with age is a response to a general increase in signal with age	28
TABLE 6: Coefficient of Variation of the harmonic amplitudes, computed from the phylogentic series in the Family Gephuroceratidae and the ontogenetic series in <u>Koenenites cooperi</u>	32
TABLE 7: Significant Correlation Coefficients (R) of variables from the study of ontogeny in <u>Koenenites cooperi</u> . Significance level is $\alpha=.05$ and $\alpha=.01$ sutural variables are HARM 1 to HARM 20 and HZERO. Aperature variables are AHARM 1 AHARM 20 and SIZE.	
TABLE 8: Varimax rotated factor matrix after rotation with Kaiser normalization, computed from six sutures and aperature shapes in the ontogenetic series of <u>Koenenites cooperi</u> . AGE is the number of volutions of the conch, SIZE is the log of the mean radius of the aperature, HARM 1 through	

TABLE 3 con't - HARM 20 are log transforms of sutural harmonic amplitudes, AHARM 1 through AHARM 20 are log transforms of aperatural Fourier harmonic amplitudes and HARMZERO is the zeroth harmonic amplitude of suture shape	37
TABLE 9: Significant Correlation Coefficients (R) of variables from the study of phylogeny in the Family Gephuroceratidae at $\alpha=.05$ and $\alpha=.01$. SEQ is the log transform of the suture's position in the phylogenetic series. HARM 1 through HARM 20 are log transforms of the Fourier harmonic amplitudes	39
TABLE 10: Varimax rotated factor matrix after rotation with Kaiser normalization, computed form the four sutures representing a phylogeneitc series in the Family Gephuroceratidae. SEQ is the log of the suture's position in the series, HARM 1 through HARM 20 are log transforms of Fourier harmonic amplitudes, and HARMZERO is the zeroth harmonic amplitude.	40

LIST OF FIGURES

		PAGE
FIGURE 1:	Variation in results, due to methods in six replications on the suture of <u>Koenenites cooperi</u>	11
FIGURE 2:	Variation in results, due to methods, in seven replications on the suture of <u>Goniatites choctawensis</u>	12
FIGURE 3:	Mean power spectra of Subclass Ammonoidea (A) and Subclass Nautiloidea (N).	17
FIGURE 4:	Mean sutures of Subclasses Nautiloidea (A) and Ammonoidea (B) and a graphic display of the difference between them (C).	18
FIGURE 5:	Power spectra of the mean suture patterns of Ammonoid Orders Anarcestida, Clymeniida, Goniatitida, and Cerititida	19
FIGURE 6:	Mean sutures of Orders Anarcestinda (A) and Clymeniida (B) and a graphic display of the difference between them (C)	20
FIGURE 7:	Mean sutures of Orders Goniatitida (A) and Cerititida (B) and a graphic display of the difference between them (C)	21
FIGURE 8:	Mean power spectra of left and right juvenile and adult sutures of <u>Acanthoclymenia neapolitana</u>	25
FIGURE 9:	Power spectra of the ontogenetic series of sutures in <u>Koenenites cooperi</u>	27
FIGURE 10:	Power spectra of the four sutres in the phylogenetic series in the Family Gephuroceratidae. SEQ 1 = <u>P. stainbrooki</u> , SEQ 3 = <u>M. sinuosum</u> , SEQ 4 = <u>K. cooperi</u> , SEQ 5 = <u>T. keyserlingi</u>	29

FIGURE 11: Contributions of harmonic frequencies seven and eighteen to the fit of the approximations of <u>Koenenites cooperi</u> at 0.5 volutions (A), 5.5 volutions (B) and a graphic display of difference between them (C).	41
FIGURE 12: Relationship between the log transforms of harmonic amplitudes seven and eighteen in the ontogenetic series in <u>K. cooperi</u>	42
FIGURE 13: Relationship between the log transforms of harmonic amplitudes seven and eighteen in the phylogenetic series in the Family Gephuroceratidae	43

INTRODUCTION

The importance of cephalopods in stratigraphy has long been recognized. The suture has been a primary character for the classification of these molluscs. In paleontology, cephalopod sutures have provided some of the classic examples of evolution by recapitulation and paedomorphosis (Tasch, p. 389, 1973).

This study provides a preliminary evaluation of the usefulness of Fourier analysis of suture patterns with respect to the higher taxonomy of the shelled cephalopods, their non-genetic norm of reaction, and their growth, development and phylogenesis.

In his discussion of leaf outlines, D'Arcy Thompson (1917) used the metaphor of a Fourier series to explain variations in form as the superposition of sinusoidal closed form waves of varying period and amplitude upon one another. He implied that plant morphogenesis and phylogeny took place as Fourier analogs. The same point could possibly be made for the ammonoid suture in paleontology, which could represent the morphogenetic superposition of sinusoidal wave forms of different amplitude and harmonic order. Because biological growth and development commonly reflect natural periodic functions, the optimal curve-fitting and filtering of many biological forms will very likely be based on the Fourier series.

Vicencio (1973) in an unpublished study attempted to use Fourier shape analysis to describe sutures. This was only a small aspect of a much larger study, and was incompletely developed. Fourier analysis has been successfully used to study the human face (Lu, 1965), the shapes of ostracodes (Younker, 1971; Kaesler and Waters, 1972; Ewald, 1975), pelecypods (Gevirtz, 1976), bryozoans (Delmet and Anstey, 1974; Anstey, Pachut and Prezbindowski, 1976), trilobites (Tuckey, 1975), blastoids (Waters, 1977), miospores (Christopher and Waters, 1974), and viruses (Crowther and Amos, 1971). The optimality of the Fourier basis of plane closed curve description has been demonstrated by Zahn and Roskies (1972).

All of the above studies, with the exception of Vicencio, were based on nonsinusoidal closed forms (i.e. complete closed curves in polar coordinates). Ammonoid sutures are natural sinusoidal curves to which the application of the Fourier series should be particularly effective.

Coefficients of variation (standard deviations divided by their means) are routinely used in biometry to compare the relative variability of different measurements. Examination of suture patterns from the widest possible taxonomic range makes it possible to calculate coefficients of variation of Fourier harmonic amplitudes at several hierarchical levels. It is then possible to compare quantitatively the degree of taxonomic variation in all of the Fourier wave forms filtered from the actual sutures. The Fourier series has the unique

property of allowing the calculation of an exact mean suture pattern for any taxonomic group, or the construction of an exact intermediate suture pattern between any two "end members".

The norm of reaction is a measure of the nongenetic, or ecophenotypic aspects of morphology. Because cephalopod sutures are bilaterally symmetrical about the mid-dorsum, available complete suture patterns provide estimations of the norm of reaction. The filtering capabilities of the Fourier series allow the subtraction of the asymmetry from the observed suture pattern, and the residual series can be used to reconstruct a more "ideal" suture pattern than that actually produced by nature.

Heterochrony implies that phylogenetic differentiation took place by extension or reduction of the development pathways followed in ontogeny. The study of heterochrony in suture patterns has previously been graphic rather than quantitative, and direct measurement of scaling factors has not been possible. The amplitudes of some Fourier wave forms vary monotonically in both ontogenetic and phylogenetic sequences. These amplitudes can be used to calculate scaling factors directly and to test the assumptions of heterochrony in the taxa studied.

METHODS

Suture shape can be estimated as Y being a function of X by a Fourier series. The general form of the Fourier equation is

$$f(x) = C_0 + \sum_{N=1}^{\infty} C_N \cos 2\pi NX/T + \sum_{N=1}^{\infty} S_N \sin 2\pi NX/T \quad (1)$$

where T equals the range of the approximation, or the period of f(x).

C_0 can be found by integrating both sides of (1) to obtain:

$$C_0 = 1/T \int_{t_0}^{t_0 + T} f(x) dx \quad (2)$$

Multiplying (1) by $\cos 2\pi NX/T$ or $\sin 2\pi NX/T$ and integrating finds C_N and S_N respectively.

$$C_N = 2/T \int_{t_0}^{t_0 + T} f(x) \cos 2\pi NX/T dx \quad (3)$$

$$S_N = 2/T \int_{t_0}^{t_0 + T} f(x) \sin 2\pi NX/T dx \quad (4)$$

A set of data points (X_i, Y_i) is approximated by a Fourier series by determining f(x) by linear interpolation over the data and solving for the Fourier coefficients in the formulas (2), (3), and (4).

Thus, if the n data points are ordered such that $X_1 < X_2 < \dots < X_n$, let $f(x) = f_i(x)$, $x_i < X < X_{i+1}$ where

$$f_i(x) = \left(\frac{Y_i - Y_{i+1}}{X_i - X_{i+1}} \right) X + \frac{-X_{i+1} + Y_i + X_i Y_{i+1}}{X_i - X_{i+1}}$$

$$X_{i-1} < X_i < X_{i+1} \quad (5)$$

$$\text{or } f_i(X) = a_i X + b_i \quad (6)$$

When $f_i(x)$ is substituted into (2)

$$C_0 = \frac{1}{X_n - X_1} \left[\int_{X_1}^{X_2} f_1(x) dx + \int_{X_2}^{X_3} f_2(x) dx + \dots + \int_{X_{n-1}}^{X_n} f_{n-1}(X) dx \right] \quad (7)$$

Integrating the functions $f_1 \dots f_n$ yields

$$C_0 = 1/(X_n - X_1) \sum_{L=1}^{n-1} \frac{a_i}{2} (X_{i+1}^2 - X_i^2) + b_i (X_{i+1} - X_i) \quad (8)$$

Similarly, for C_N and S_N

$$C_N = \frac{2}{X_n - X_1} \sum_{j=1}^{n-1} \int_{X_j}^{X_{j+1}} (a_i X + b_i) \cos \frac{2\pi NX dx}{T}, N=1, 2, 3, \dots \quad (9)$$

$$S_N = \frac{2}{X_n - X_1} \sum_{i=1}^{n-1} \int_{X_i}^{X_{i+1}} (a_i X + b_i) \sin \frac{2\pi NX dx}{T}, N=1, 2, 3, \dots \quad (10)$$

Integrating, these become

$$C_N = \sum_{i=1}^{n-1} \frac{a_i}{\pi N} \left[X_{i+1} \sin \frac{2\pi NX_{i+1}}{T} - X_i \sin \frac{2\pi NX_i}{T} \right] + \frac{b_i}{\pi N} \left[\sin \frac{2\pi NX_{i+1}}{T} - \sin \frac{2\pi NX_i}{T} \right] + \frac{a_i T}{2\pi^2 N^2} \left[\cos \frac{2\pi NX_{i+1}}{T} - \cos \frac{2\pi NX_i}{T} \right] \quad (11)$$

$$\begin{aligned}
S_N = & \sum_{i=1}^{n-1} - \frac{a_i}{\pi N} \left[y_{i+1} \cos \frac{2\pi NX_{i+1}}{T} - X_i \cos \frac{2\pi NX_i}{T} \right] \\
& - \frac{b_i}{\pi N} \left[\cos \frac{2\pi NX_{i+1}}{T} - \cos \frac{2\pi NX_i}{T} \right] \\
& + \frac{a_i}{2\pi N^2} \left[\sin \frac{2\pi NX_{i+1}}{T} - \sin \frac{2\pi NX_i}{T} \right]
\end{aligned} \tag{12}$$

Equations (8), (11) and (12) were coded into program FOURIER (Appendix A) and used to compute Fourier approximations of suture shape. Harmonic amplitudes (A_N) and phase angles (Φ_N) are calculated by the formulae:

$$A_N = C_N^2 + N^2$$

$$\Phi_N = \text{TAN}^{-1} \frac{SN}{CN}$$

Published suture diagrams were the source of all data (Appendix B). Diagrams were photographically enlarged and then digitized on a set of cartesian coordinates. Each suture pattern was situated to have the venter lie along the abscissa. The origin was at the point at which the suture pattern and venter cross. Forty to one hundred X, Y coordinates of points on the suture pattern were recorded, starting at the origin and finishing with the point at which the suture intersected the mid-dorsum. Points were selected at regular intervals, with exceptions for inclusion of finer details which would

otherwise have been smoothed over by linear interpolation over the sampling interval. Two methods of treating this data were then compared.

The first or "half suture" method shifted the orientation of the suture pattern with respect to the coordinate system so that both the first and last data points had a Y-values were multiplied by the same normalization constant in order to maintain scale relationships. The Fourier series approximation was then computed over the 0.0 to 2π interval.

The second method takes advantage of the bilateral symmetry of the suture patterns by constructing a mirror image from the mid-dorsum on around to the venter. This "complete suture" is then normalized, as before, to range from 0.0 to 2π from venter to venter. The Fourier series approximation is then calculated over this interval.

A data set consisting of 126 suture patterns was used for comparative evaluation of the two methods. For each method, twenty harmonic amplitudes and twenty phase angles were computed from each suture pattern. Data sets of less than forty one data points were eliminated from analysis because of the Nyquist frequency limitations (Davis, 1973, p. 266). Because each harmonic amplitude was computed from the residual signal (that not accounted for by the previous harmonics), all harmonics are orthogonal. The contribution of each harmonic to the approximation of the original data by the Fourier series was first delineated by computing its root mean square error, as defined by the formula:

$$\text{RMS} = \sqrt{\frac{\sum_{j=1}^N (Y_j - \hat{Y}_j)^2}{N-1}}$$

where N is the number of data points, Y_j is the Y -value of the j th data point and \hat{Y}_j is the approximation of the Y -value of the j th data point.

\hat{Y}_j is computed by the formula:

$$\hat{Y}_j = A_0 + \sum_{i=1}^F (A_i \sin (i X_j + \Phi_i))$$

where A_0 is the value of the zeroth harmonic amplitude, A_i is the value of the i th harmonic amplitude, and Φ_i is the phase angle of the i th harmonic, and F is the highest harmonic frequency calculated.

Significance testing was carried out using an analysis of variance design associated with Snedecor's F -test (Mendenhall, 1968, p. 174-181). Although data points were not necessarily spaced at equal intervals, which is necessary for a rigorous test of significance, their close approximation to equal intervals still allows the use of the significance test as an accurate estimate of true significance (Gevirtz, 1976).

Subroutine FTEST (Appendix A) was used to compute both the root mean square error and the F -statistics. It was found with both methods that all twenty harmonics contributed significant ($\alpha = .05$) shape information.

It was also found that with the computation of twenty harmonic amplitudes, the complete suture method was able to

reduce root mean square error to less than an arbitrary value of 0.05 in 80% of the cases (101 out of 126); whereas the half suture method could achieve this level of accuracy in only 75% of the cases (95 out of 126).

The complete suture method also concentrates more information in the harmonic amplitudes. Because a suture pattern is bilaterally symmetrical, the coefficients of the sine terms in the Fourier equation take on a value of zero (Lu, 1965). Consequently, the Fourier series becomes a cosine series and the phase angles only have values of plus or minus ninety degrees.

A further advantage of the full suture method over the half suture method lies in the assumption of a repeating signal inherent in a Fourier series approximation (Davis, p. 256-272). A suture pattern repeats itself by virtue of its continuity around the conch from the venter to the mid-dorsum and back to the original point, the venter. The half suture method ignores the assumption of a repeating signal. It also changes the function by rotating the orientation of the sutures on the coordinate system, so it can not lend itself to representation of the morphogenesis of the sutures as well as the complete suture method. Therefore, only the results of the complete suture method have been presented in this paper.

It should be also be noted that the results obtained from the complete suture method agree with those reported by Vicencio (1973). This includes his observation that Schindewolf's phylogenetic scheme (1954) of trilobate, quadrilobate and quinquelobate primary sutures correspond with large contributions

to the fit of the Fourier series approximation by the fourth, sixth and eighth harmonics, respectively.

The sutures of the ammonitoid ammonites are too complex to be studied directly by Fourier analysis. The lobules and folioles which create the intricate nature of the suture patterns cause the functions describing them to be multivalued. The Fourier series cannot deal with this problem (Ehrlich and Weinberg, 1970). Many of the ceratitic and goniatitic sutures also exhibit this degree of complexity. A possible solution to this problem, not examined in this study, would be the use of an iterative curve smoothing algorithm. Vicincio (1973) attempted such analysis, but found it not particularly useful for extremely complex sutures. However, for sutures such as those in Schistoceras missouriense, which only have a few multivalued points along the ordinate, such a procedure could be used. The number of iterations required to make the curve suitable for Fourier analysis should be retained as an additional variable measuring complexity. A table of ammonoid taxa which have been studied is included in Appendix C.

In order to evaluate the reproducibility of results by this method, multiple data sets were generated from two suture drawings, one of Koenenites cooperi and one of Goniatites choctawensis. The data sets were processed, and results were compared by graphical display (Figures 1 and 2) and by computing the coefficients of variation:

$$CV_n = 100.0 (\sigma_n / \mu_n)$$

FIGURE 1: Variation in results, due to methods
in six replications on the suture of
Koenenites cooperi.

FIGURE 2: Variation in results, due to methods,
in seven replications on the suture
of Goniatites choctawensis.

where n is the harmonic frequency number, σ is the standard deviation and μ is the mean.

The graphs of the harmonic amplitudes vs. the harmonic frequency number (power spectra) of the six repetitions of K. cooperi (Figure 1) show a large variation of the harmonic amplitudes at harmonic frequencies eleven and fourteen, The coefficient of variation has maxima of 66.64 and 69.83 at these respective frequencies (Table 1). The seven replications of G. choctawnsis (Figure 2) and K. cooper (Figure 1) is that relative variations increases greatly as the harmonic amplitude drops below 10^{-2} . This threshold level can be lowered by reducing random noise due to methods. More accurate digitizing equipment (accuracy greater than .025 in.) or greater enlargement of suture patterns (larger than 8×10 photographs) can increase the signal strength with respect to noise.

RESULTS

A data set of 140 sutures was analyzed and the mean harmonic amplitudes were calculated for the portion of the taxonomic hierarchy sampled (Appendix D). In order to compare the degree of taxonomic variation in the Fourier was forms, the coefficients of variation (CV_n) was also computed for taxonomically hierarchical levels (Appendix E). Table 2 gives the mean coefficients of variability within hierarchical levels. Harmonic frequency four shows a relatively constant CV, with a minimum of 38.21 and a maximum of 45.19. The second

TABLE 1: Values of the Coefficient of Variation (CV) for six replications of Koenenites copperi and seven replications of Goniatites choctawensis.

HARMONIC FREQUENCY	COEFFICIENT OF VARIATION	
	<u>K. cooperi</u>	<u>G. choctawensis</u>
1	2.46	4.51
2	2.78	4.53
3	3.26	7.60
4	2.61	21.28
5	1.99	70.09
6	3.15	1.15
7	6.42	3.90
8	1.33	46.07
9	4.17	20.92
10	4.54	4.04
11	66.64	1.99
12	16.36	4.42
13	4.30	15.78
14	69.83	5.82
15	13.77	13.69
16	8.68	124.66
17	16.09	4.88
18	8.04	15.26
19	37.38	8.03
20	32.87	20.31

TABLE 2: Mean values for the Coefficient of Variability computed for the taxonomic hierarchy.

<u>HARMONIC</u>	<u>GENERA</u>	<u>FAMILIES</u>	<u>SUPERFAMILIES</u>	<u>ORDERS</u>
1	46.74	45.79	31.23	20.30
2	41.30	42.94	35.86	35.57
3	42.19	60.73	52.01	41.08
4	39.70	44.26	38.21	45.19
5	57.37	56.35	37.21	55.11
6	32.02	32.84	48.83	50.60
7	44.85	38.33	47.61	52.76
8	28.70	65.84	43.29	53.92
9	36.27	40.94	45.49	63.33
10	43.40	46.78	54.75	48.26
11	35.74	67.27	46.55	53.96
12	48.37	61.85	27.53	55.59
13	51.81	59.39	45.42	65.94
14	56.64	49.45	47.19	59.01
15	42.29	54.16	35.04	62.79
16	43.04	47.64	51.07	58.16
17	44.21	35.02	64.74	72.05
18	40.30	45.76	52.90	59.58
19	42.61	38.42	44.35	52.93
20	54.93	44.49	36.39	59.91

harmonic also has a constant CV, ranging from 35.57 to 42.94. Table 2 shows that all harmonic frequencies (1-20) contribute shape information at all levels in the taxonomic hierarchy.

The complexity of a suture pattern can be roughly quantified as the number of harmonic frequencies required to reduce root mean square error to 0.05 or less. The average number to reduce RMS to 0.05 or less is seven for the nautiloids and eleven for the ammonoids. Those ammonoid approximations which could not reduce RMS to 0.05 were not included in the computation of this average.

Sixteen harmonics were the maximum number required to reduce RMS to 0.05 or less in the nautiloids. The ammonoids differ from the nautiloids primarily in the increased signal of the higher order harmonics (Figures 3 and 4). This is an expected result of the ammonoids' increase in sutural complexity by the addition of lateral lobes, which are not found in the nautiloids.

The mean power spectrum of the Subclass Ammonoidea was computed from the four power spectra shown in Figure 5. These are the mean harmonic amplitudes of the Orders Anarcestida, Clymeniida, Goniaticitida and Cerititida. The mean suture patterns which these power spectra represent were redrawn by FORTRAN program FILTER (Appendix F) and are presented in Figures 6 and 7). Discriminant analysis (Nie, et al., 1975, p. 434-467) was performed using these four Orders as the classification categories. Only nine individuals out of 129 were

FIGURE 3: Mean power spectra of Subclass Ammonoidea (A) and Subclass Nautiloidea (N).

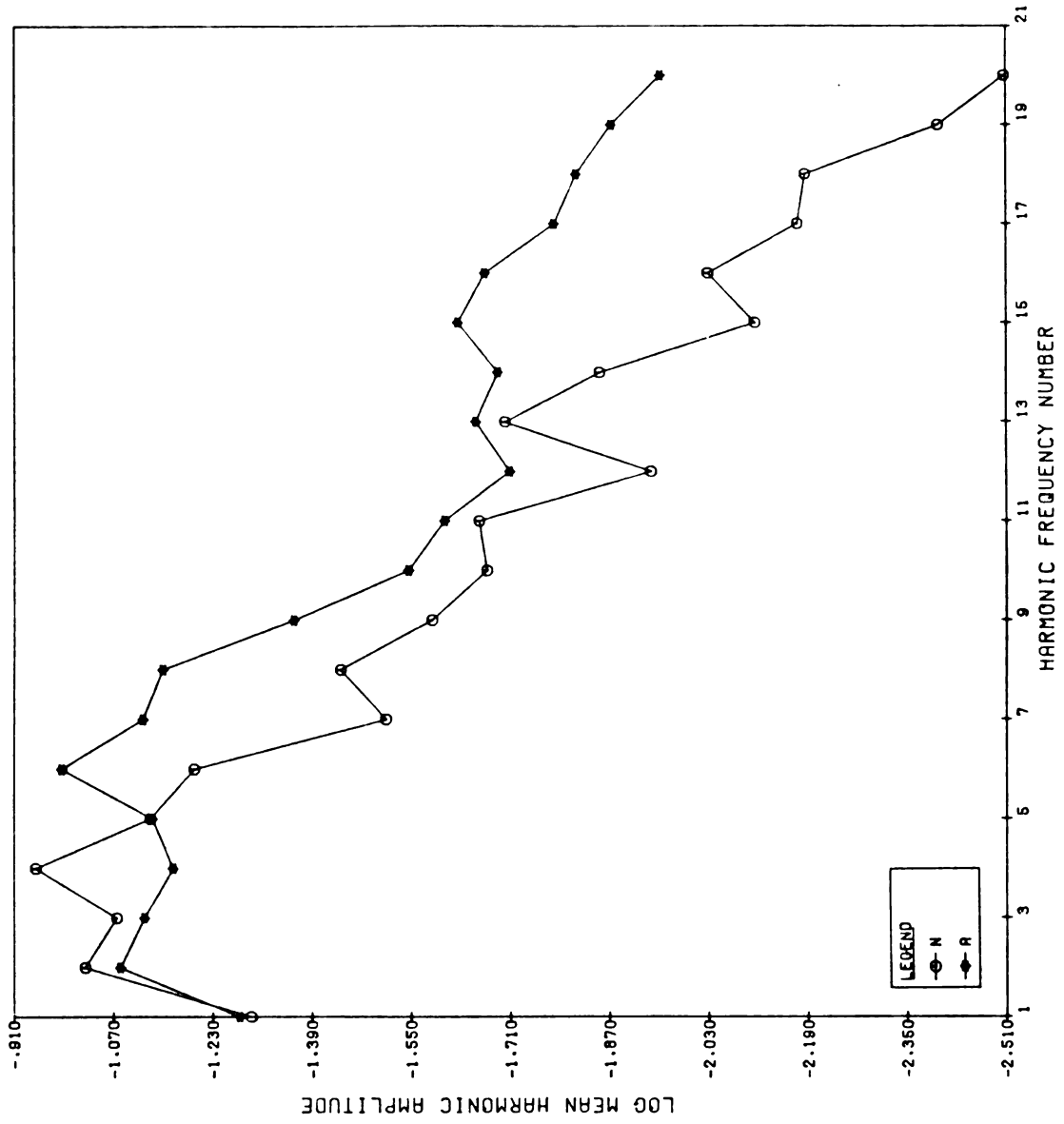


FIGURE 4: Mean sutures of Subclasses Nautiloidea (A) and Ammonoidea (B) and a graphic display of the difference between them (C).

FIGURE 5: Power spectra of the mean suture patterns of Ammonoid Orders Anarcestida, Clymeniida, Goniaticitida, and Cerititida.

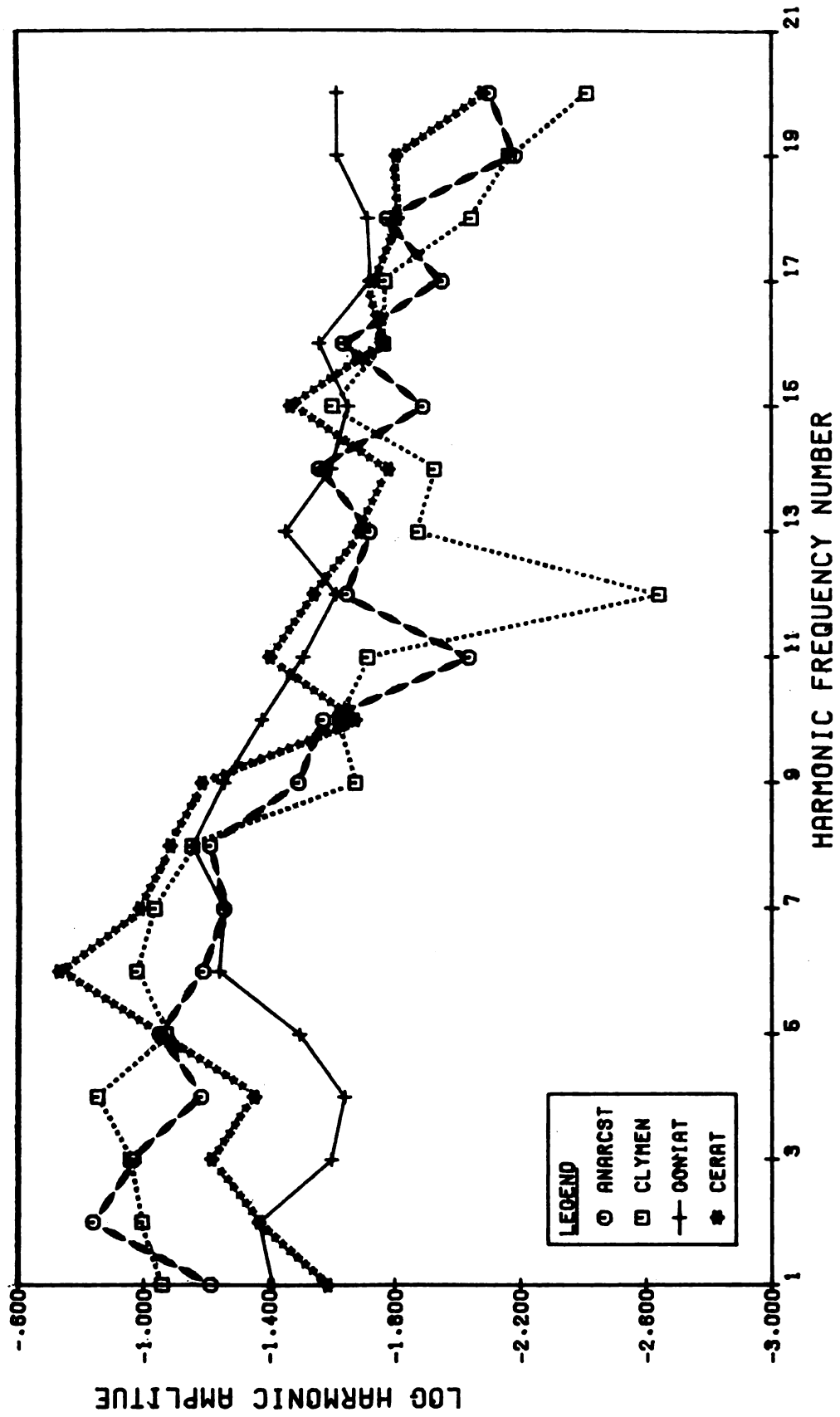


FIGURE 6: Mean sutures of Orders Anarcestinda (A) and Clymeniida (B) and a graphic display of the difference between them (C).

FIGURE 7: Mean sutures of Orders Goniaticida (A) and Cerititida (B) and a graphic display of the difference between them (C).

misclassified (Table 3). This result is significant at $\alpha = .01$ with $\chi^2 = 318.35$. The sensitivity of Fourier shape analysis to genetic differences at high taxonomic levels is demonstrated by the above results.

The ability to filter nongenetic effects from the morphologic information, leaving only genetically regulated shape information, is of great importance to the studies of taxonomy, ontogeny, and phylogeny. The data set included only two complete suture patterns suitable for examining both halves. Both suture patterns were of Acanthoclymenia neapolitana, at $2\frac{1}{2}$ volutions of the conch and at maturity.

Each suture half was processed eight to ten times. Discriminant analysis was performed upon the harmonic amplitudes and 100% correct classification ($\chi^2 = 105.00$) was achieved (Table 4). The significant differences between left and right suture halves are summarized in the mean power spectra of these sutures (Figure 8). These differences are not discernible in visual inspection of the suture patterns.

The ontogenetic sequences of suture patterns of Adrianites dunbari, Agatherisis uralicum and Koenenites cooperi (taken from Arkell, et al., 1957) were studied. Suture patterns which were too complex for analysis i.e., those which require a double valued function) were omitted. Sutural complexity, as measured by the number of harmonics required to reduce RMS to 0.05 or less, increased with age in each of the three sequences. Because of the elimination of the complex mature sutures of A. dunbari and A. Uralicum, further study of ontogeny was limited to K. cooperi.

TABLE 3: Summary of Discriminant Analysis of data from sutures in the Orders Anarcestinda, Clymeniida, Goniatiida, and Ceratitida.

ACTUAL GROUP NAME	N OF CASES	PREDICTED GROUP MEMBERSHIP			
		ANARCESTINDA	CLYMENIIDA	GONIATIDA	CERATITIDA
Anarcestinda	44	41.0	2.0	1.0	0.0
		93.2%	4.5%	2.3%	0.0%
Clymeniida	13	3.0	10.0	0.0	0.0
		23.1%	76.9%	0.0%	0.0%
Goniatiida	50	2.0	0.0	47.0	1.0
		4.0%	0.0%	94.0%	2.0%
Ceratitida	22	0.0	0.0	0.0	22.0
		0.0%	0.0%	0.0%	100.0%

TABLE 4: Summary of Discriminate Analysis of data from Acanthoclymenia neapolitana. Perfect discrimination between left and right suture halves in both juvenile and adult sutures demonstrates presence of nongenetic influences on suture shape.

ACTUAL GROUP NAME	N OF CASES	PREDICTED GROUP MEMBERSHIP			
		L-JUVENILE	R-JUVENILE	L-ADULT	R-ADULT
L-JUVENILE	8	3.0 100.0%	0.0 0.0%	0.0 0.0%	0.0 0.0%
R-JUVENILE	10	0.0 0.0%	10.0 100.0%	0.0 0.0%	0.0 0.0%
L-ADULT	8	0.0 0.0%	0.0 0.0%	8.0 100.0%	0.0 0.0%
R-ADULT	9	0.0 0.0%	0.0 0.0%	0.0 0.0%	9.0 100.0%

FIGURE 8: Mean power spectra of left and right
juvenile and adult sutures of
Acanthoclymenia neapolitana.

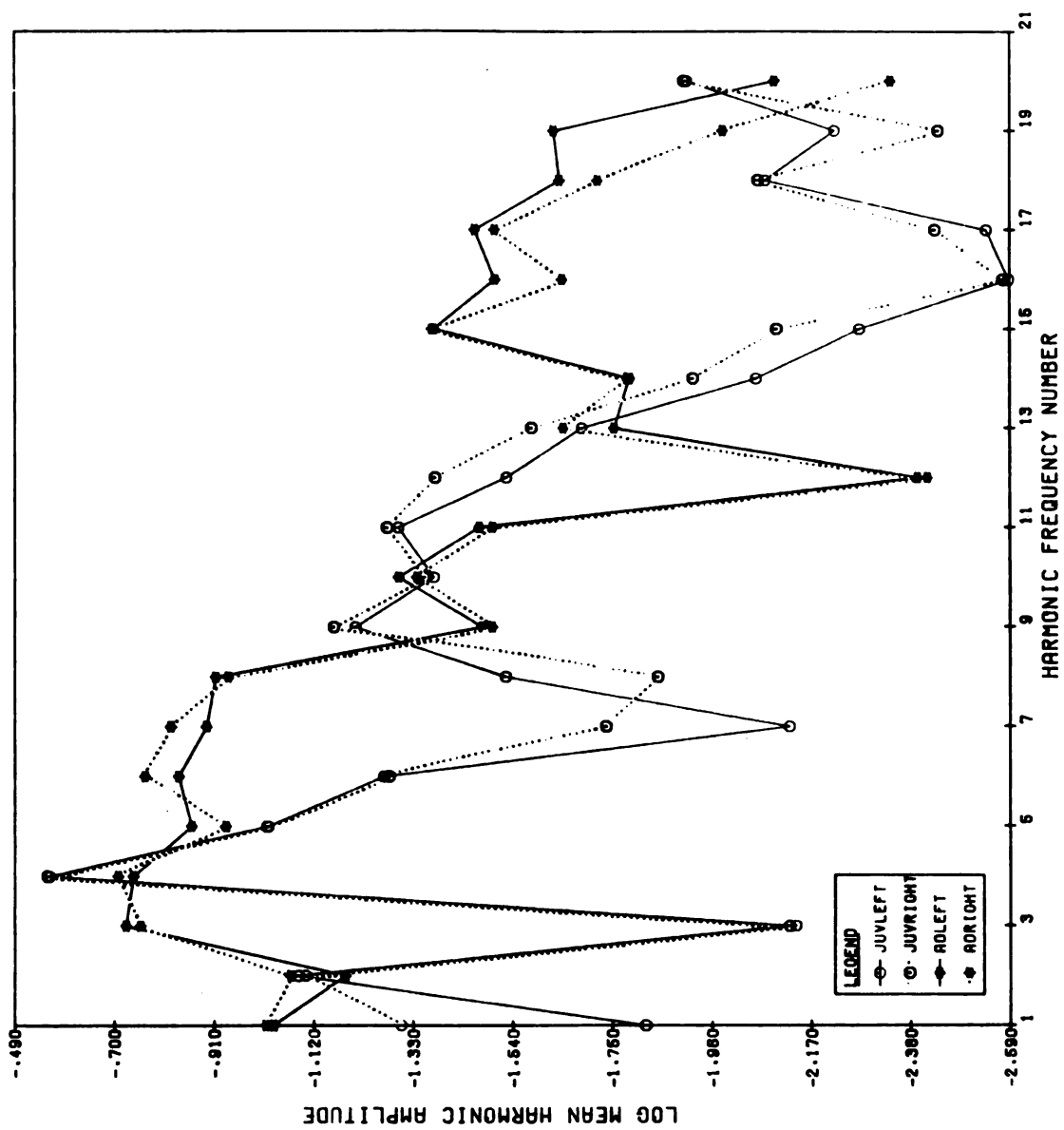


Figure 9 is the power spectra of the harmonic amplitudes of the six sutures in the ontogenetic series of K. cooperi as reported by Miller (1938). Growth and development is reflected in the power spectra as a slow broadening and migration of the first peak of the series to higher order harmonic frequencies. Each successive approximation (i.e., suture) tends to be of a higher overall power spectrum than the previous one. This visual observation is supported by ranking the approximation at each frequency and summing the ranks over the approximations (Table 5). The above observation fit Miller's description of the ontogeny as proceeding by the subdivision of lobes and increase in size.

A phylogenetic sequence of sutures proposed by Miller (Arkell, et al. p. 134, 1957) for the Family Gephuroceratidae was studied in the same manner as the ontogeny of sutures in K. cooperi. The sequence consisted of Ponticeras aequabilis, Manticoceras simulator, Manticoceras sinuosum, Koenenenites cooperi and Timanites keyserlingi. The complete sutures of M. simulator was not available in the literature and could not be included. The same problem forced substitution of Ponticeras stainbrooki for P. aequabilis.

P. stainbrooki, which has the most simple suture, forming only four distinct lobes (Arkell et al., p. 135, 1957), has a peak in its power spectrum (Figure 10) at the fourth harmonic frequency and then drops for the higher order frequencies. M. sinuosum, K. cooperi and T. keyserlingi should then be expected to have peaks at frequencies six, eight and ten,

FIGURE 9: Power spectra of the ontogenetic series of sutures in Koenenites cooperi.

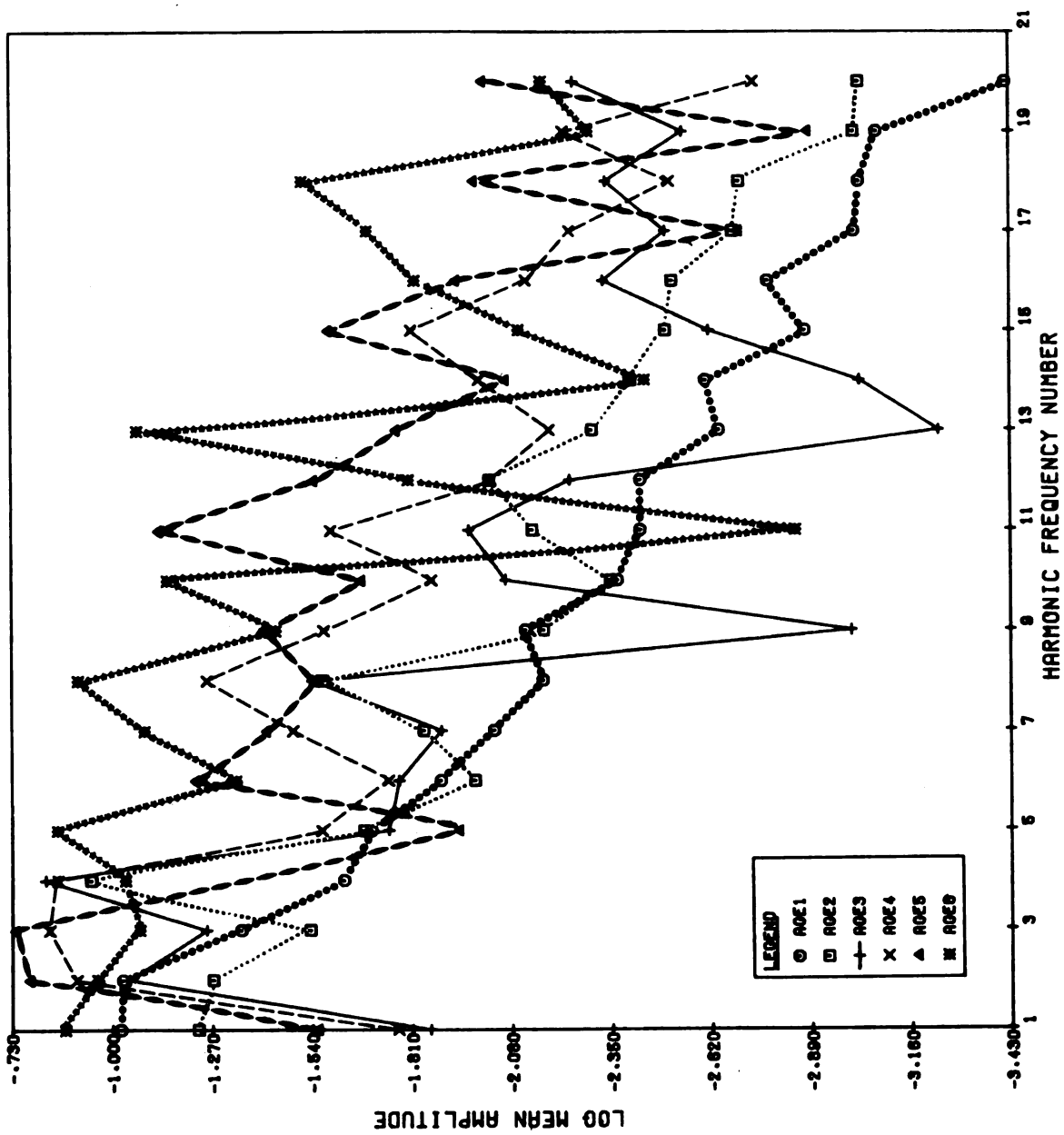
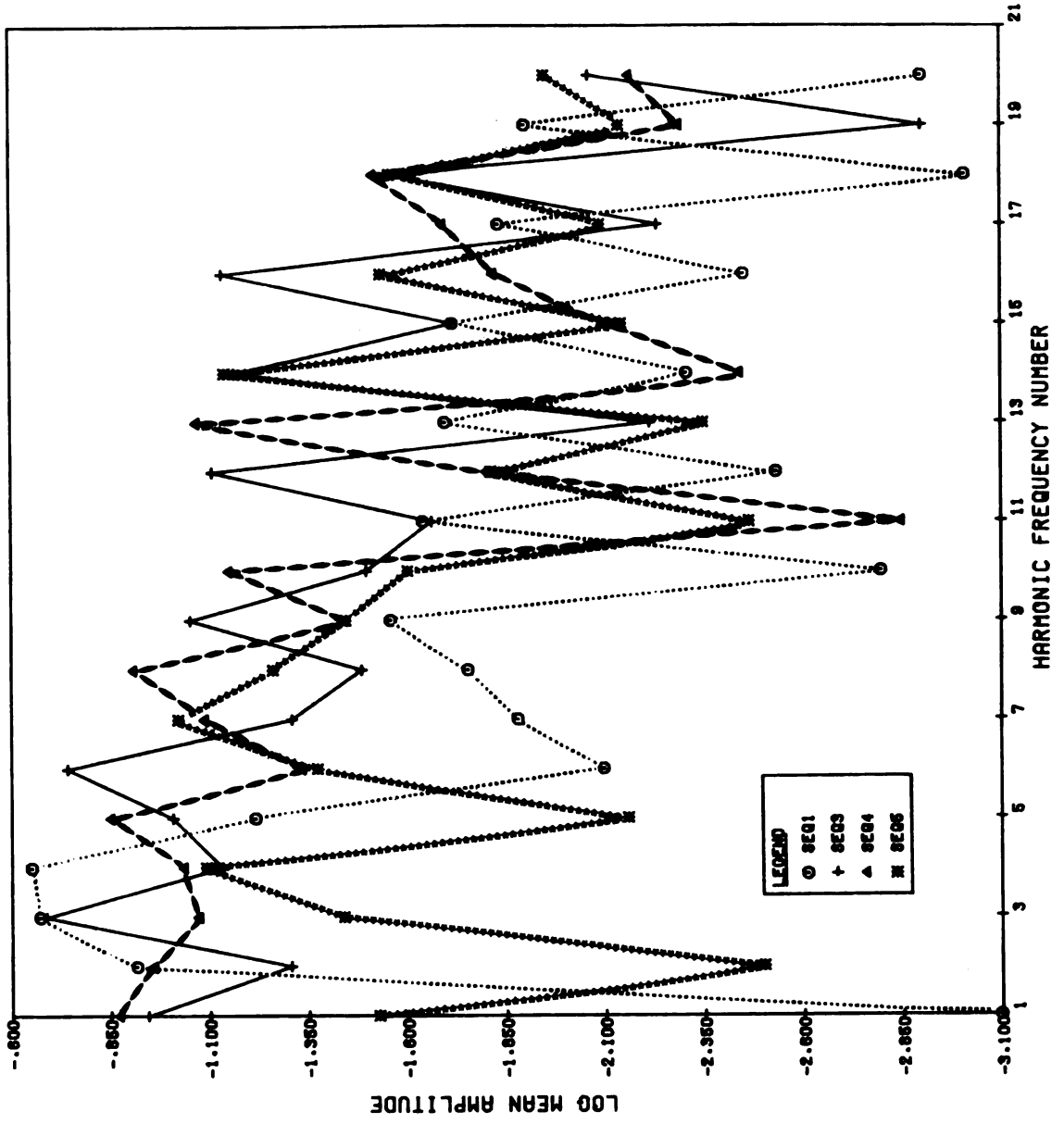


TABLE 5: Rankings of the harmonic amplitudes within each harmonic frequency for six suture patterns in the ontogenetic series of Koenenites cooperi. The increase in rank sums with age is a response to a general increase in signal with age.

HARMONIC NUMBER	VOLUION OF CONCH					
	0.5	1.5	2.5	3.5	4.5	5.5
	RANKINGS OF HARMONIC AMPLITUDES					
1	5	4	1	2	3	6
2	3	1	2	5	6	4
3	2	1	3	5	6	4
4	1	3	6	4	5	2
5	3	4	2	5	1	6
6	2	1	3	4	6	5
7	1	3	2	4	5	6
8	1	2	4	5	3	6
9	3	2	1	4	6	5
10	1	2	3	4	5	6
11	2	3	4	5	6	1
12	1	3	2	4	6	5
13	2	3	1	4	5	6
14	2	4	1	6	5	3
15	1	3	2	5	6	4
16	1	2	3	4	5	6
17	1	3	4	5	2	6
18	1	2	4	3	5	6
19	1	2	4	3	5	6
20	<u>1</u>	<u>2</u>	<u>4</u>	<u>3</u>	<u>6</u>	<u>5</u>
Ranking Sums	35	50	56	87	95	97

FIGURE 10: Power spectra of the four sutures in the phylogenetic series in the Family Gephuroceratidae. SEQ1 = P. stainbrooki
SEQ3 = M. sinuosum, SEQ4 = K. cooperi,
SEQ5 = T. keyserlingi



corresponding to their respective number of lobes (Arkell et al., p. 135, 1957). M. sinuosum and K. cooperi do have high values where expected, but these are not their maxima T. keyserlingi has a relatively low value for its tenth harmonic amplitude. These anomalies are considered to be the results of combinations of lower order frequencies making good approximations to the fit of the data, leaving less residual signal to be accounted for by the higher order frequencies. The asymmetric, non-regular (variable frequency) nature of the lobes of T. keyserlingi can be better approximated by the combination of two signals, the fourth and the seventh harmonic frequencies, than by the tenth frequency.

A measure of the similarity of the sutures within a grouping can be made by calculating the normalized roughness coefficient (RC) of each suture pattern.

$$RC_j = \sqrt{\frac{1}{20} \sum_{i=1}^{20} (A_{ij} / \bar{A}_i)}$$

where A_{ij} is the harmonic amplitude of the i th frequency in the j th suture, and \bar{A}_i is the mean harmonic amplitude of the i th frequency.

A set of identical sutures should all have values of RC equal to 10 or 3.1623. The phylogenetic sequence has value of RC ranging from 2.9135 for T. keyserlingi to 4.7666 for M. sinuosum. The ontogenetic sequence ranges from 1.6082 at the earliest suture to 7.4351 at the adult suture. This indicates that the sutures of the phylogenetic series are less different from each other than those of the ontogenetic series.

The sources of the variation can be determined by examining the coefficients of variability for the two sequences (Table 6). The phylogenetic sequence only has two values of CV greater than 100 (harmonics twelve, thirteen). Other sources of variation are, in descending order, harmonics six, fourteen, sixteen, eleven, and one. The ontogenetic sequence has six harmonics with coefficients of variability greater than 100. Only harmonics one, two, four, six, twelve, fourteen and sixteen have lower values of CV in the ontogenetic sequence than in the phylogenetic sequence. The extremely low values of CV for harmonics two and four in the ontogenetic series indicate that these harmonic frequencies are relatively independent of development, and reflect a basic sutural form that does not vary with growth.

Log transforms of the harmonic amplitudes from the suture patterns of the ontogenetic series were submitted to principal components factor analysis (Nye, et al., p. 468-514, 1970). The number of volutions of the conch at each suture was included as a variable representing age. Also included were log transforms of the size of the aperture and twenty harmonic amplitudes computed in closed form (Ehrlich and Weinberh, 1970; Ewald, 1975; Anstey, Pachut and Prezbindowski, 1976) from the shape of the aperture at the respective number of volutions.

The matrix of correlations, output as a preliminary result, shows significant ($\alpha = .05$) correlations of age with size, sutural harmonic frequencies zero, six, seven, ten,

TABLE 6: Coefficients of Variation of the harmonic amplitudes, computed from the phylogentic series in the Family Gephuroceratidae and the ontogenetic series in Koenenites cooperi.

<u>HARMONIC NUMBER</u>	<u>COEFFICIENT OF VARIATION</u>	
	Phylogeny	Ontogeny
1	80.14	76.61
2	67.25	32.53
3	56.67	61.68
4	52.41	39.45
5	64.15	114.58
6	95.35	68.16
7	52.95	78.82
8	70.77	84.23
9	51.54	76.68
10	76.93	113.23
11	80.68	123.17
12	104.56	67.60
13	113.84	153.60
14	88.63	66.56
15	43.61	93.68
16	87.28	65.48
17	46.38	117.06
18	55.36	119.19
19	62.38	71.61
20	52.28	81.46

twelve, sixteen, eighteen, twenty and aperatural harmonic frequencie four (Table 7). All of these variables load most heavily on the first principal component (Table 8) or the general growth factor (Gould, 1966).

Principal components analysis of the phylogenetic se-
quence was performed using a dummy "SEQ" variable coded as
the log of the suture's position in the series. As before,
log transforms of the harmonic amplitudes were used. No
aperatural shapes were available for the study. Only har-
monic frequencies seven, eighteen and twenty were signifi-
cantly ($\alpha = .05$) correlated with "SEQ" (Table 9). These four
variables all loaded most highly on Factor two (Table 10).

The correlation of harmonic frequencies seven and eigh-
teen with age in both the ontogenetic and the phyloeneetic
series is an interesting point. The seventh harmonic is re-
sponsible, in part, for the presence of lateral lobes. The
eighteenth harmonic frequency is equivalent to eighteen evenly
spaces lobes. Alone, its effect can only be in small scale
sculpturing of the suture patterns. However, the high levels
of correlation imply an interaction of the two variables.
The results of this interaction is demonstrated by Figure 11,
which shows the actual contribution of harmonic frequencies
seven and eighteen to the approximation of the earliest and
adult sutures of K. cooperi.

The log transformation of the two harmonic amplitudes
were plotted against each other and regression lines were com-
puted (Figures 12 and 13) for the ontogenetic and phylogenetic
data. The slopes of the regression lines are 0.593 for the

TABLE 7: Significant Correlation Coefficients (R) of variables from the study of ontogeny in *Koenenites cooperi*. Significance level is $\alpha=.05$ and $\alpha=.01$ (*) Sutural variables are HARM 1 to HARM 20 and HZERO. Aperatural variables are AHARM 1 to AHARM 20 and SIZE.

AGE		SIZE	
Size	.97982*	HARM 6	.82005
HARM 6	.88217	HARM 7	.97274*
HARM 7	.85522	HARM 8	.89910
HARM 10	.86423*	HARM 9	.98817*
HARM 12	.81744	HARM 16	.95864*
HARM 16	.99448*	HARM 17	.88508
HARM 18	.95072*	HARM 18	.95433*
HARM 20	.85268	AHARM 2	-.82488
AHARM 4	.87485	AHARM 4	.83539
HZERO	.84909		
HARM 1		HARM 2	
AHARM 1	-.95539*	HARM 3	.94236*
AHARM 8	-.92109*		
AHARM 9	-.95587*	HARM 3	
AHARM 12	-.94688*	HARM 15	.88907
AHARM 13	-.83069		
AHARM 17	-.90256	HARM 5	
AHARM 18	-.85346	HARM 17	.86010
HARM 4		AHARM 2	-.92246
AHARM 3	.92283*		
AHARM 7	.99258*	HARM 7	
AHARM 11	.95408*	HARM 8	.86530
AHARM 16	.91773*	HARM 10	.95855
HZERO	.85889	HARM 13	.89130
HARM 6		HARM 16	.94243*
HARM 7	.81684	HARM 17	.82926
HARM 10	.86140	HARM 18	.89193
HARM 12	.82726		
HARM 16	.86628		
HARM 18	.86439		
HARM 20	.81644		

TABLE 7 cont.

HARM 8			HARM 9		
HARM	10	.82804	HARM	13	.88184
HARM	16	.85520	HARM	14	.87175
HARM	17	.95015*			
HARM	18	.81873			
HARM	19	.82126			
HZERO		.83168			
HARM 10			HARM 11		
HARM	16	.93151*	AHARM	1	.83761
HARM	17	.85613	AHARM	5	-.90542
HARM	18	.95146*	AHARM	12	.88750
AHARM	2	-.83102	AHARM	17	.87568
HARM 12			HARM 15		
HARM	15	.87466	HARM	16	.83718
HARM	16	.84243	AHARM	16	.82249
AHARM	16	.83725	HZERO		.89209
HARM 16			HARM 17		
HARM	18	.92970*	HARM	19	.86686
HARM	20	.87048	AHARM	2	-.85699
AHARM	3	.84199			
AHARM	4	.88852			
AHARM	16	.86241			
HZERO		.89209			
HARM 18			HARM 20		
HARM	20	.88226	AHARM	3	.88562
AHARM	4	.83301	AHARM	4	.91223
AHARM	10	-.84336	AHARM	16	.82590
			HZERO		.82147

TABLE 7 cont.

AHARM 1
 AHARM 8 .95857*
 AHARM 9 .90245
 AHARM 12 .97886*
 AHARM 13 .89945
 AHARM 17 .96507*
 AHARM 18 .95515*
 AHARM 19 .87201

AHARM 3
 AHARM 4 .88997
 AHARM 7 .95938
 AHARM 13 .87177
 AHARM 16 .95328*
 HZERO .96608*

AHARM 4
 AHARM 13 .83189
 HZERO .91379

AHARM 5
 AHARM 15 .88451

AHARM 7
 AHARM 11 .91470
 AHARM 16 .93642*
 HZERO .90564

AHARM 8
 AHARM 9 .93093
 AHARM 12 .88597
 AHARM 13 .81726
 AHARM 17 .88752
 AHARM 18 .93639*
 AHARM 19 .92850*

AHARM 9
 AHARM 12 .86207
 AHARM 17 .84155

AHARM 11
 AHARM 16 .81148

AHARM 12
 AHARM 13 .87988
 AHARM 17 .95505*
 AHARM 18 .89848

AHARM 13
 AHARM 17 .91031
 AHARM 18 .94541*
 AHARM 19 .84781
 HZERO .82988

AHARM 16
 HZERO .92995*

AHARM 17
 AHARM 18 .93180*
 AHARM 19 .85166

AHARM 18
 AHARM 19 .95388*

TABLE 8: Varimax rotated factor matrix after rotation with Kaiser normalization, computed from six sutures and aperature shapes in the ontogenetic series of *Koenenites cooperi*. AGE is the number of volutions of the conch, SIZE is the log of the mean radius of the aperature, HARM 1 through HARM 20 are log transforms of sutural harmonic amplitudes, AHARM 1 through AHARM 20 are log transforms of aperatural Fourier harmonic amplitudes and HARMZERO is the zeroth harmonic amplitude of suture shape.

VARIABLE	FACTOR 1	FACTOR 2	FACTOR 3	FACTOR 4	FACTOR 5
AGE	.93095	.12358	.20427	.24324	.14349
SIZE	.91106	-.01845	.33936	.20075	.12937
HARM 1	.04744	-.96428	.00810	.08370	.24400
HARM 2	.38867	.48005	.04720	.47221	.62443
HARM 3	.48821	.55092	.07665	.58349	.32955
HARM 4	.63106	.56751	-.04265	-.07006	-.52932
HARM 5	.47613	-.56974	.66233	.01727	.02644
HARM 6	.81542	.10494	-.10269	.24554	.48296
HARM 7	.86909	-.08695	.26030	.40387	.08719
HARM 8	.82918	.00204	.45977	.12207	-.28927
HARM 9	.45442	-.21971	-.02623	.83580	.15598
HARM 10	.83008	-.05777	.33333	.19589	.27659
HARM 11	.04819	.78985	.48791	.34308	-.08229
HARM 12	.84305	.08704	-.34431	.38136	-.02437
HARM 13	.70816	-.45177	.05469	.51865	.10417
HARM 14	.24374	.07420	-.16513	.92276	-.14674
HARM 15	.66461	.38480	-.10043	.62194	-.02868
HARM 16	.92899	.19943	.16573	.25684	.08233
HARM 17	.72833	-.13196	.65750	.05715	-.12109
HARM 18	.96917	-.02102	.15318	-.02483	.19091
HARM 19	.49499	.28506	.79095	.11655	-.10309
HARM 20	.88390	.39724	-.02688	-.15448	.16117

TABLE 8 cont.

VARIABLE	FACTOR 1	FACTOR 2	FACTOR 3	FACTOR 4	FACTOR 5
AHARM 1	.07594	.99248	-.10260	-.01231	.00123
AHARM 2	-.74069	.54285	-.37975	-.00355	-.06994
AHARM 3	.77361	.60047	.04071	.05069	-.19045
AHARM 4	.78512	.48999	.34254	-.03190	.14805
AHARM 5	-.04403	-.57678	.71519	-.17988	.33002
AHARM 6	.29771	.10473	.23780	-.03688	.86090
AHARM 7	.68660	.58229	.01347	-.06836	-.43637
AHARM 8	-.12455	.97500	.00779	-.10929	.14571
AHARM 9	-.32268	.93259	-.00799	-.02309	-.15593
AHARM 10	-.89914	.34432	.14784	.01185	.13002
AHARM 11	.46937	.53744	-.26477	-.13152	-.63422
AHARM 12	.15714	.95297	-.21968	.01577	-.14088
AHARM 13	.43500	.88713	.14407	-.00746	.12287
AHARM 14	.17055	.54760	.71788	-.23370	.23000
AHARM 15	.10404	-.16289	.81163	-.27572	.45676
AHARM 16	.84401	.38254	-.05828	.15272	-.33548
AHARM 17	.15635	.95794	-.05140	.23358	-.01679
AHARM 18	.21100	.94908	.03214	-.02827	.22837
AHARM 19	.03030	.89695	.20024	.01361	.39233
AHARM 20	.25705	.63451	.26431	-.59475	-.20262
HARMZERO	.76763	.52393	.24738	.19344	-.19397

TABLE 9: Significant Correlation Coefficients (R) of variables from the study of phylogeny in the Family Gephuroceratidae at $\alpha=.05$ and $\alpha=.01(*)$. SEQ is the log transform of the suture's position in the phylogenetic series. HARM 1 through HARM 20 are log transforms of the Fourier harmonic amplitudes.

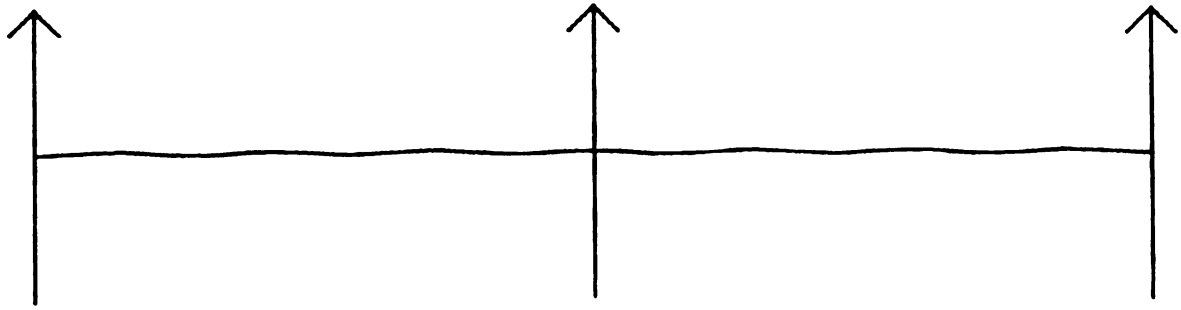
	SEQ	
HARM 7	.99742*	
HARM 18	.95574	
HARM 20	.96331	
	HARM 1	
HARM 10	.98079	
HARM 18	.96335	
	HARM 4	
HARM 18	-.97937	
	HARM 6	
HARM 12	.99829*	
HARM 16	.96995	
	HARM 7	
HARM 18	.95070	
	HARM 9	
HARM 19	-.98345	
	HARM 10	
HARM 18	.96978	
	HARM 12	
HARM 16	.97012	
HARM 19	-.95463	
	HARM 14	
HARM 17	-.95408	
HZERO	-.99793*	
	HARM 17	
HZERO	.96656	
	HARM 18	
HARM 20	.97393	

TABLE 10: Varimax rotated factor matrix after rotation with Kaiser normalization, computed from the four sutures representing a phylogenetic series in the Family Gephuroceratidae. SEQ is the log of the suture's position in the series, HARM 1 through HARM 20 are log transforms of Fourier harmonic amplitudes, and HARMZERO is the zeroth harmonic amplitude.

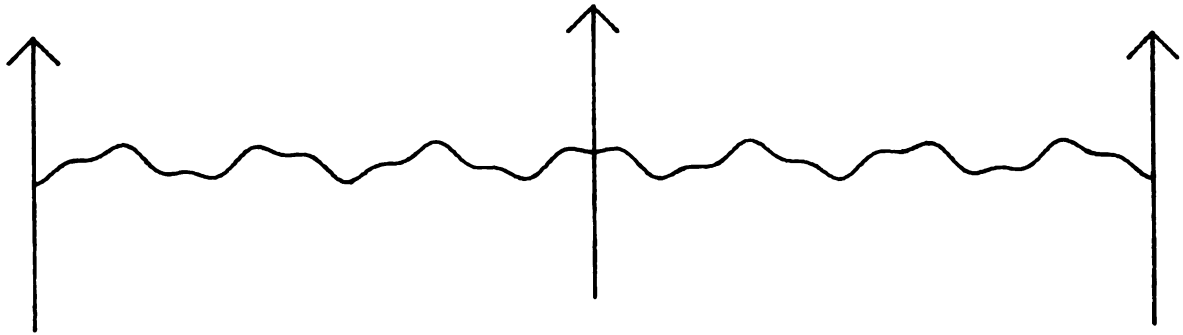
VARIABLE	FACTOR 1	FACTOR 2	FACTOR 3
SEQ	.46889	.84657	-.25708
HARM 1	.80022	.59156	.09034
HARM 2	.01218	-.46439	.87535
HARM 3	.19196	-.87878	.42148
HARM 4	-.77523	-.56903	.27186
HARM 5	.35566	-.31327	.86779
HARM 6	.96505	.21535	-.15494
HARM 7	.44470	.87560	-.19579
HARM 8	.23334	.91280	.31783
HARM 9	.96230	-.22026	-.15694
HARM 10	.66822	.73571	.10482
HARM 11	.08710	-.96333	-.23045
HARM 12	.97243	.16059	-.17435
HARM 13	-.23329	.22795	.93484
HARM 14	.51499	.01546	-.85997
HARM 15	.16449	-.97662	.09033
HARM 16	.88527	.25251	-.38537
HARM 17	-.58465	.26344	.76419
HARM 18	.69944	.70027	-.13667
HARM 19	-.99434	.09952	.02443
HARM 20	.64945	.67044	-.35770
HARMZERO	-.56325	.01434	.82892

FIGURE 11: Contributions of harmonic frequencies seven and eighteen to the fit of the approximations of Koenenites cooperi at 0.5 volutions (A), 5.5 volutions (B) and a graphic display of the difference between them (C).

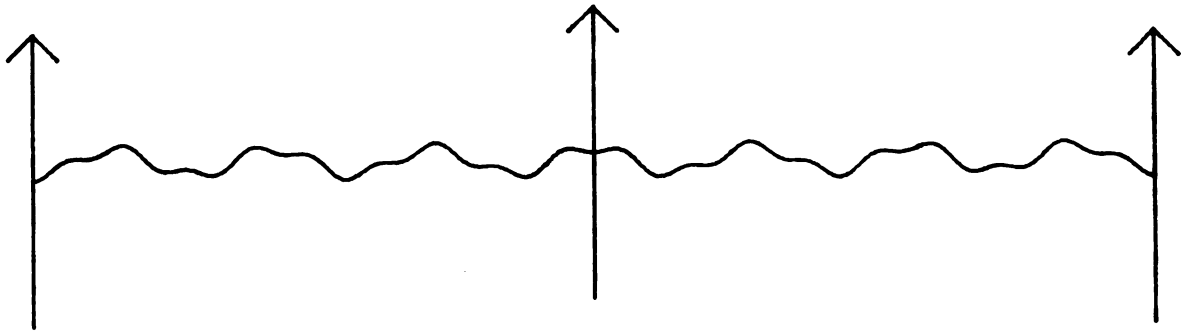
41a



A



B



C

FIGURE 12: Relationship between the log transforms of harmonic amplitudes seven and eighteen in the ontogenetic series in K. cooperi.

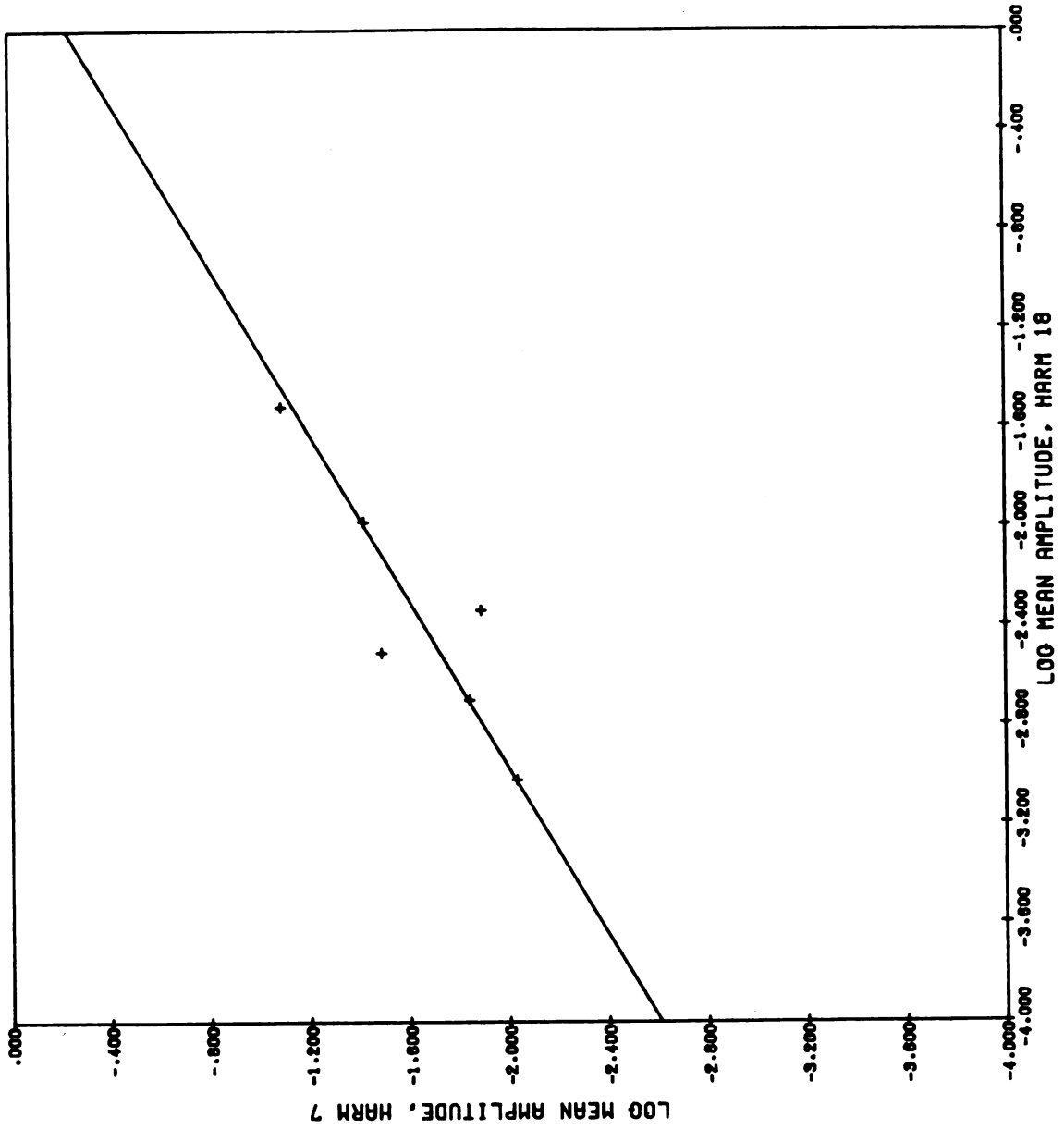
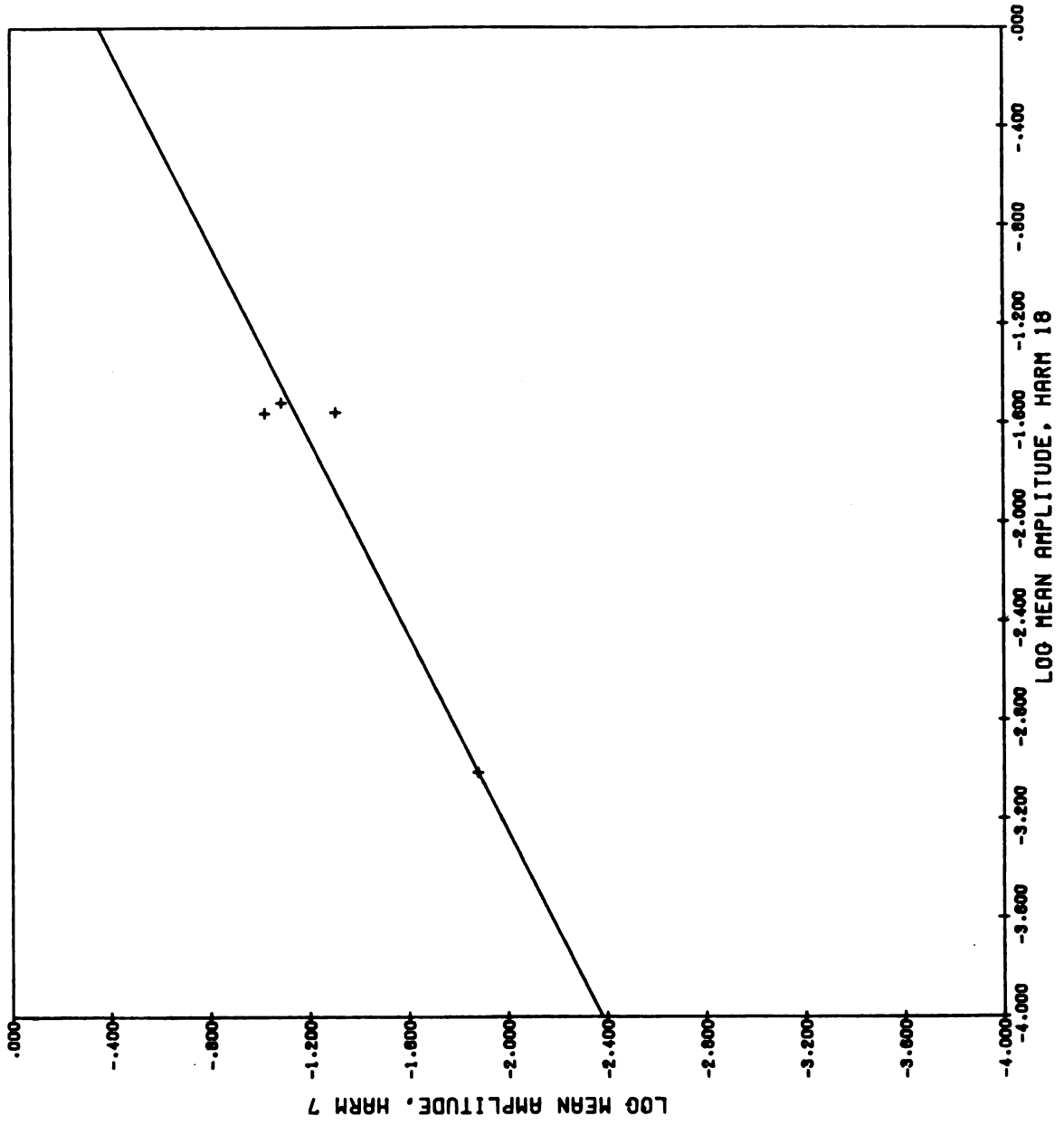


FIGURE 13: Relationship between the log transforms of harmonic amplitudes seven and eighteen in the phylogenetic series in the Family Gephuroceratidae.



ontogenetic sequence and 0.505 for the phylogenetic sequence. This difference is slight enough to show that the two harmonics maintain a constant relationship through the changes of ontogeny and that this relationship is held constant across the changes of the specific phylogenetic sequence postulated by Miller. The constant relationship demonstrates, on a quantitative level, the assumption of heterochrony (in this example, recapitulation) in the cephalopods analyzed.

SUMMARY AND CONCLUSIONS

A wide taxonomic range of cephalopod suture patterns have been studied by means of the Fourier series. Coefficients of variation and mean suture patterns have been computed. The filtering capability of the Fourier series allows the quantitative comparison of these meansuture patterns, at any level in the taxonomic heirarchy. This same filtering capability permits a measure of a suture's nongenetic norm or reaction. Measurements show that subtle differences exist between the left and right suture halves of Acanthoclymenia neapolitana at both $2\frac{1}{2}$ volutions of the conch and at maturity.

The relationship between harmonic frequency seven and harmonic frequency eighteen is monotonic for both an ontogenetic and a phylogenetic sequence in the family Gephuroceratidae. The linear relationships were calculated directly from the log transformation of the harmonic amplitudes and found to be almost identical. Heterochrony (recapitulation) is there fore demonstrated on a quantitative level for

Koenenites cooperi and three other genera to which it is closely related. The correlation of aperatural shape variables, generated by Fourier analysis, with those of sutural shape through development in K. cooperi implies a functional relationship between specific aspects of aperature and suture morphology.

The power of Fourier analysis in the study of the cephalopod suture is unprecedented. Taxonomy, nongenetic norm of reaction, heterochrony, and functional morphology of cephalopod sutures can be studied quantitatively by means of Fourier analysis.

LIST OF REFERENCES

- Anstey, R.L., J.F. Pachut, and D.R. Prezbindowki, Morphogenetic gradients in Paleozoic bryozoan colonies: *Paleobiology*, V. 2, No. 2, p. 131-146.
- Arkell, W.J., et al., 1957, *Treatise on Invertebrate Paleontology: part L, Mollusca 4*, University Kansas Press, 490 p.
- Christopher, R.A., and J.A. Waters, 1974, Fourier series as a quantitative descriptor of miospore shape: *Jour. Paleontology*, V. 48, No. 4, p. 697-709.
- Crowther, R.A., and L.A. Amos, 1971, Harmonic analysis of electron microscope images with rotation symmetry: *J. Mol. Biol.*, V. 60, No. 1, p. 123-130.
- Davis, J.C., 1973, *Statistics and data analysis in geology*: John Wiley and Sons, Inc., New York, 550 p.
- Delmet, D.A., and R.L. Anstey, Fourier analysis of morphological plasticity within an Ordovician bryozoan colony: *Jour. Paleontology*, V. 48, No. 2, p. 217-226.
- Ehrlich, R. and B. Weinberg, 1970, An exact method for characterization of grain shape: *J. Sed. Petrology*, V. 40, No. 1, p. 205-212.
- Ewald, F.C., 1975, Feasibility of completely automated microfossil identification in petroleum exploration: Mich. State University, MS Thesis, 68 p.
- Gevirtz, J.L., 1976, Fourier analysis of Bivalve Outlines: Implications on evolution and autecology: *Math. Geol.*, V. 8, No. 2, p. 151-163.
- Gould, S.J., 1966, Allometry and size in ontogeny and phylogeny: *Biol. Rev.*, V. 41, No. 4, p. 587-640.
- Kaesler, R. and Waters, J.A., 1972, Fourier analysis of the Ostracode margin: *Geol. Soc. Amer. Bull.*, V. 83, No. 4, p. 1169-1178.
- Lu, K.H., 1965, Harmonic analysis of the human face: *Biometrics*, V. 21, No. 2, p. 491-505.

- Mendenhall, W., 1968, Introduction to linear models and the design and analysis of experiments: Wadsworth Publishing Co., Inc., Belmont, CA, 465 p.
- Miller, A.K., 1938, Devonian ammonoids of America: Geol. Soc. Amer. Spec. Paper 14, 262 p.
- Nie, N.H., C.H. Hull, J.G. Jenkins, K. Steinbrenner, and D.H. Bent, 1975, Statistical package for the social sciences: McGraw-Hill Book Co., Inc., New York, 675 p.
- Oxnard, C., 1973, Form and pattern in Human evolution: some mathematical physical, and engineering approaches: Univ. Chicago Press, 218 p.
- Schindewolf, O.H., 1954, On development, evolution and terminology of the ammonoid suture line: Harvard Univ. Mus. Comp. Zool., Bull. 112, No. 3, p.217-237.
- Tasch, P., 1973, Paleobiology of the invertebrates, data retrieval from the fossil record: John Wiley and Sons, Inc., New York, 946 p.
- Thompson, D.W., 1917, On growth and form: Cambridge University Press.
- Tuckey, M., 1975, Sexual dimorphism in the Devonian trilobite *Phacops rana*: Mich. State University, MS Thesis, 90 p.
- Vicencio, R., 1973, Models for the morphology and morphogenesis of the ammonoid shell: McMaster Univeristy, Ph. D. Dissertation, 116 p.
- Waters, J.A., 1977, Quantification of shape by use of Fourier analysis: The Mississippian Blastoid genus *Pentremites*: Paleobiology, V. 3, No. 3, p. 288-299.
- Younker, J.K., 1971, Evaluation of the utility of two-dimensional Fourier shape analysis for the study of ostracode carapaces: Michigan State University, MS Thesis, 62 p.
- Zahn, C.T., and R.Z. Roskies, 1972, Fourier descriptors for plane closed curves: IEEE Trans. on Computers C-21, No. 3. p. 269-282.

APPENDIX A

```

PROGRAM FOURIER(TAPE60,OUTPUT,PUNCH,TAPE14,TAPE61=OUTPUT)
C----- THIS PROGRAM COMPUTES THE FOURIER SERIES OF HARMONIC SUTURE
C----- PATTERNS. INPUT DATA CAN BE UP TO 100 (X,Y) COORDINATES
C----- STARTING AT THE POINT XMIN=J, Y=0.
C----- TWENTY HARMONICS ARE CALCULATED AND THE OUTPUT
C----- IS IN PUNCHED CARDS AND PRINTED OUTPUT.
C----- TAPE14 IS AN ALTERNATE OUTPUT FILE WHICH HAS
C----- ONLY NAMES AND HARMONIC AMPLITUDES (NO STATISTICS
C----- OR PHASE ANGLES). PHASE ANGLES ARE ONLY OUTPUT ON
C----- FILE PUNCH.
C
C----- THE FIRST CARD OF EACH SAMPLE MUST BE A TITLE CARD,
C----- STARTING IN COLUMN 2. DATA FORMAT IS (F5.2,1X,F5.2)
C----- THE FIRST DATA POINT MUST BE (0.0,0.0)
C----- END OF SAMPLE DATA IS INDICATED BY AN EOR.
COMMON/DATA/X(200),Y(200),AMP(20),FAZE(20)
DIMENSION NAME(7),C(20),D(20)
DATA PI,PISQ/3.14159,9.86960/
C----- READ INPUT DATA FROM TAPE60
1000 NP=0
      READ(60,1) NAME
      IF(EOF(60)) 999,15
15    NP=NP+1
      READ(60,2) X(NP),Y(NP)
      IF(EOF(60)) 20,15
10    IF(Y(NP).GT.50.0) Y(NP)=Y(NP)-101.0
      GO TO 15
20    NP=NP-1
      IF(NP.LT.41) GO TO 900
C----- ORDER DATA FROM X=XMIN TO X=XMAX
      N=NP
      ISORT=0
      DO 40 I=2,N
      IF(X(I).GT.X(I-1)) GO TO 40
      T=X(I) ; X(I)=X(I-1) ; X(I-1)=T
      T=Y(I) ; Y(I)=Y(I-1) ; Y(I-1)=T
40    ISORT=1
      CONTINUE
      N=N-1
      IF(ISORT.GT.J) GO TO 30
      NPM1=NP-1
      PRINT 7,NAME
C----- CONSTRUCT SECOND HALF OF SUTURE PATTERN
      DO 100 I=1,NPM1
100   X(NP+I)=X(NP)+X(NP)-X(NP-I)
      Y(NP+I)=Y(NP)-Y(NP-I)
      NP=NP+NPM1
      NPM1=NP-1
C----- NORMALIZE DATA TO RANGE FROM X=0 TO X=2PI
      T=6.28318/X(NP)
      DO 200 I=1,NP
200   Y(I)=Y(I)*T
      X(I)=X(I)*T
C----- COMPUTE FOURIER SERIES
      T=6.28318
      C0=0.0
45    DO 45 N=1,20
      C(N)=C(N)=0.0
      DO 60 I=1,NPM1
      A=(Y(I)-Y(I+1))/(X(I)-X(I+1))
      B=(X(I)+Y(I+1)-X(I+1)+Y(I))/(X(I)-X(I+1))
      C0=C0+(X(I+1)**2+A/2.+(X(I+1)-X(I))*B
      DO 50 N=1,20
      W=FLOAT(N)
      XN=X(I) * XN1=X(I+1)
      C(N)=C(N)+A*T*(SIN(W*XN1)-SIN(W*XN))/(2.*PISQ**N**2)
      *-A * (XN1*COS(W*XN1)-XN*COS(W*XN))/(PI*N)
      *-B * (COS(W*XN1)-COS(W*XN))/(PI*N)
      D(N)=D(N)+A*T*(COS(W*XN1)-COS(W*XN))/(2.*PISQ**N**2)
      **A * (XN1*SIN(W*XN1)-XN*SIN(W*XN))/(PI*N)
      **B * (SIN(W*XN1)-SIN(W*XN))/(PI*N)
50    CONTINUE
60    CONTINUE
      C0=C0/T
      DO 65 N=1,20
      AMP(N)=SQRT(C(N)**2+D(N)**2)
      FAZE(N)=ATAN2(D(N),C(N))

```

```

110
120
130
140
150
160
170
180
190
200
210
220
230
240
250
260
270
280
290
300
310
320
330
340
350
360
370
380
390
400
410
420
430
440
450
460
470
480
490
500
510
520
530
540
550
560
570
580
590
600
610
620
630
640
650
660
670
680
690
700
710
720
730
740
750
760
770
780
790
800
810
820
830
840
850
860
870

```

55	CONTINUE	44
	PUNCH 1, NAME	45
	PUNCH 2, CG	46
	PUNCH 3, AMP	47
	PUNCH 4, FAZE	48
	WRITE (14, 3) NAME, CG	49
	WRITE (14, 4) AMP	50
	CALL FTEST(NP, CG)	51
	GO TO 1000	52
900	PRINT 9, NAME	53
	GO TO 1000	54
999	STOP	55
1	FORMAT(1X, 7A10)	56
2	FORMAT(F5.2, 1X, F5.2)	57
3	FORMAT(10X, 7A10, F10.5)	58
4	FORMAT(10X, 15F7.4/10X, 15F7.4)	59
6	FORMAT(10F7.4/10F7.4/10F7.4)	60
7	FORMAT(1H0, 7A10)	61
8	FORMAT(5F10.5)	62
9	FORMAT(*L INSUFFICIENT DATA FOR *7A10)	63
	END	64

```

SUBROUTINE FTEST(L,AG)
COMMON/ DATA/X(200),Y(200),AMP(20),FAZE(20)
DIMENSION YNEW(200),F(20),FMS(20)
INTEGER DFD(20)
LM1=L-1
NP=(L+1)/2
C----- INITIALIZE SSE2
SSE2=0.0
DO 10 J=1,L
C----- INITIALIZE YNEW TO THE VALUE OF THE ZEROITH HARMONIC
YNEW(J)=A0
C----- COMPUTE SUM OF SQUARED ERROR OF A0 FROM ORIGINAL DATA
SSE2=SSE2+(Y(J)-A0)**2
10 CONTINUE
DO 20 I=1,20
C----- COMPUTE NEW APPROXIMATION WITH THE ADDITION OF HARMONIC I
DO 20 J=1,L
YNEW(J)=YNEW(J)+AMP(I)*SIN(I*X(J)+FAZE(I))
20 CONTINUE
C----- MAKE OLD #MODEL 2# INTO NEW #MODEL 1#
SSF1=SSE2
C----- INITIALIZE SSE2
SSE2=0.0
C----- COMPUTE DEGREES OF FREEDOM FOR THE DENOMINATOR
DFD(I)=NF-I-1
C----- DEGREES OF FREEDOM FOR THE NUMERATOR ALWAYS = ONE
C
C----- COMPUTE SUM OF SQUARED ERROR OF NEW APPROXIMATION
C----- FROM ORIGINAL DATA
DO 30 J=1,L
SSC2=SSE2+(Y(J)-YNEW(J))**2
30 CONTINUE
C----- COMPUTE ROOT MEAN SQUARE ERROR
RMS(I)=SQRT(SSC2/LM1)
C----- COMPUTE F-STATISTIC
F(I)=(SSF1-SSE2)/(SSC2/DFD(I))
50 CONTINUE
PRINT 1,AG
PRINT 2,AMP
PRINT 3,RMS
PRINT 4,DFD
PRINT 5,F
1 FORMAT(1H+,T71,10HZEROITH HARMONIC =,F1),5)
2 FORMAT(2H HARMONIC AMPLITUDES#T25,15F7.4/24X,15F7.4)
3 FORMAT(2H ROOT MEAN SQUARE ERROR#T25,15F7.3/24X,15F7.3)
4 FORMAT(2H DEGREES FREEDOM DENOM.#T25,15(I,F,2X)/24X,15(I,F,2X))
5 FORMAT(2H F - RATIOS#T25,15F7.2/24X,15F7.2)
END

```

```

1190
1100
1110
1120
1130
1140
1150
1160
1170
1180
1190
1200
1210
1220
1230
1240
1250
1260
1270
1280
1290
1300
1310
1320
1330
1340
1350
1360
1370
1380
1390
1400
1410
1420
1430
1440
1450
1460
1470
1480
1490
1500
1510
1520
1530
1540
1550
1560

```

APPENDIX B

APPENDIX B

Sources of Suture Diagrams

- Arkell, W.J., et al., 1957, Treatise on Invertebrate Paleontology, part L, Mollusca 4, University Kansas Press, 490 p.
- Miller, A.K., 1947, Tertiary Nautiloids of the Americas, Geol. Soc. Amer., Mem. 23, 234 p.
- Miller, A.K. and W.M., Furnish, 1940, Permian Ammonoids of the Guadalupe mountain region and adjacent areas, Geol. Soc. Amer., Spec. paper 26, 242 p.
- Petersen, M.S., 1975, Upper Devonian (Famennian) ammonoids from the Canning Basin, western Australia, Paleontological Society, Mem. 8, 55p.
- Teichert, C., et al., 1964, Treatise on Invertebrate Paleontology, part K, Mollusca 3, University Kansas Press, 519 p.

APPENDIX C

APPENDIX C

Taxonomy of Ammonoids Studied

Subclass Ammonoidea

Order Anarcestida

Superfamily Anarcestaceae

Family Mimoceratidae

Subfamily Mimoceratinae

Genus Gyroceratites

species gracilis

Family Agoniatitidae

Genus Agoniaties

species vanuxemi

species costulatus

Family Anarcestidae

Subfamily Anarcestinae

Genus Anarcestes

species lateseptatus

Genus Subanarcestes

species macrocephalus

Genus Werneroceras

species ruppachensis

species plebeiforme

Superfamily Prolobitaceae

Family Prolobitidae

Subfamily Prolobitinae

Genus Prolobites

species delphinus

Superfamily Pharcicerataceae

Family Gephuroceratidae

Genus Manticocerasspecies sinuosumGenus Ponticerasspecies aequabilisGenus Koenenitesspecies cooperiGenus Timanitesspecies keyserlingi

Order Clymeniida

Superfamily Gonioclymeniaceae

Family Acanthoclymeniidae

Genus Acanthoclymeniaspecies neopolitana

Superfamily Clymeniaceae

Family Clymeniidae

Genus Platyclymeniaspecies annulataGenus species americanaspecies polypleura

Order Goniatitida

Superfamily Cheilocerataceae

Family Tornoceratidae

Genus Tornocerasspecies crebriseptumspecies delepinei

Family Cheiloceratidae

Subfamily Cheiloceratinae

Genus Cheilocerasspecies schmidtispecies ovatumspecies angulatum

species enkebergense

Subfamily Raymondiceratinae

Genus Raymondiceras

species simplex

Subfamily Speradoceratinae

Genus Sporadoceras

species milleri

Subfamily Imitoceratinae

Genus Imitoceras

species rotatorium

Superfamily Agathicerataceae

Family Agathiceratidae

Genus Agathiceras

species uralicum

Superfamily Cyclolobaceae

Family Popanoceratidae

Subfamily Marathonitinae

Genus Peritrochia

species dieneri

Superfamily Goniatitaceae

Family Goniatitidae

Subfamily Goniatitinae

Genus Goniatites

species choctawensis

Genus Muensteroceras

species parallelum

Subfamily Girtyoceratinae

Genus Eumorphoceras

species bisulcatum

Family Neococeratidae

Genus Pseudoparalegoceras
species russienseGenus Atsabites
species multiliratus

Family Schistoceratidae

Subfamily Schistoceratinae

Genus Paralegoceras
species iowenseGenus Diaboloceras
species varicostatumGenus Winslowoceras
species henbesti

Superfamily Adrainitaceae

Family Adrianitidae

Subfamily Adrianitinae

Genus Adrianites
species dunbariGenus Texoceras
species texanum

Subfamily Dunbaritinae

Genus Emilites
species incertus

Order Cerititida

Superfamily Otocerataceae

Family Xenodiscidae

Genus Xenodiscites
species waageniGenus Xenaspis
species skinneri
species carbonaria

Genus Paraceltites

species elegans

species ornatus

species hoeferi

species altudensi

APPENDIX D

APPENDIX D

Mean Harmonic Amplitudes of the Taxonomic Hierarchy

Subclass Bacritoidea

Order Bacritida

Family Bictritidae

.02095 .32555 .02070 .01040 .04330 .01150 .02130 .00450 .01120 .00305
 .00935 .00265 .00640 .00240 .00245 .00070 .00405 .00040 .00305 .00195

Genus Bacrites

.0234 .0280 .0228 .0167 .0239 .0045 .0079 .0020 .0052 .0001
 .0060 .0030 .0042 .0009 .0007 .0008 .0030 .0007 .0024 .0001

Genus Lobobacrities

.0182 .3711 .0186 .0041 .0627 .0185 .0347 .0070 .0172 .0060
 .0127 .0023 .0086 .0039 .0042 .0006 .0051 .0003 .0037 .0038

Subclass Nautiloidea

Order Nautilida

Superfamily Nautilaceae

.05106 .09448 .08412 .11349 .07427 .06311 .03092 .03661 .02606 .02124
 .02187 .01156 .01988 .01398 .00786 .00936 .00671 .00652 .00398 .00311

Family Nautilidae

Genus Nautilus

species pompilius

.07480 .17710 .13065 .08930 .04245 .01360 .02030 .02565 .00220 .01850
 .00915 .00410 .00835 .00750 .00340 .00240 .00035 .00015 .00175 .00240

Family Hercoglossidae

.04712 .04751 .04583 .08717 .07846 .08613 .03662 .03354 .02610 .00884
 .02081 .01162 .01160 .00790 .00879 .00863 .00199 .00249 .00289 .00150

Genus Hercoglossa

.07885 .03910 .07132 .08622 .06632 .14175 .05500 .01477 .03080 .00718
 .00770 .00643 .01133 .00573 .00467 .00352 .00302 .00463 .00235 .00289

Genus Aturoidea

species paucifex

.00270 .00450 .01850 .15030 .14680 .07740 .04910 .09520 .03590 .01380
 .0711 .03450 .02640 .01850 .02170 .02450 .00330 .00110 .00750 .00030

Genus Cimonia species vincenti

.03280 .06190 .01510 .04010 .03520 .05430 .01890 .00890 .01750 .00490
.00010 .00260 .00330 .00450 .00500 .00320 .00000 .00280 .00020 .00120

Genus Deltoidonautilus

.07414 .08453 .07840 .07205 .06550 .07107 .02349 .01528 .02018 .00948
.00435 .00295 .00537 .00287 .00378 .00330 .00165 .00143 .00152 .00153

Family Aturiidae
Genus Aturia

.03125 .05883 .07588 .16400 .10190 .08960 .03583 .05065 .04988 .03638
.03565 .01895 .03970 .02655 .01138 .01705 .01778 .01693 .00730 .00543

Subclass Ammonoidea
Order Anarcerstida

.06117 .14496 .10793 .06543 .08882 .06464 .05544 .06138 .03219 .02717
.00918 .02262 .01919 .02774 .01292 .02331 .01125 .01687 .00658 .00796

Superfamily Anarcestaceae

.05883 .22808 .07480 .07541 .03812 .03812 .03677 .02476 .01534 .01787
.01432 .01206 .00986 .01067 .00861 .00786 .00670 .00685 .00538 .00591

Family Mimocertidae
Subfamily Minoceratinae
Genus Gyroceratitites
species gracilis

.02220 .31423 .01930 .00470 .03897 .02253 .02480 .01633 .01433 .01177
.01087 .00800 .00680 .00530 .00343 .00343 .00320 .00330 .00233 .00257

Family Agoniatitidae

.08849 .26273 .16612 .12352 .01078 .07081 .04357 .04184 .01772 .02550
.01334 .01602 .01341 .01124 .00124 .01210 .00903 .00975 .00728 .00867

Family Anarcestidae
Subfamily Anarcestinae

.06580 .10728 .03898 .09803 .04061 .02103 .04193 .01610 .01398 .01634
.01874 .01215 .00938 .01296 .01115 .00804 .00788 .00750 .00653 .00649

Superfamily Prolobitaceae
Family Prolobitidae
Subfamily Prolobitinae
Genus Prolobites
species delphinus

.03740 .1532 .1359 .0353 .1513 .0612 .0504 .0858 .0239 .0239
.0067 .0132 .0141 .0203 .0184 .0244 .0162 .0164 .0092 .0081

Superfamily Pharcicerataceae
Family Gephuroceratidae

.08729 .05360 .11310 .08559 .08504 .09459 .07916 .07359 .05732 .03973
.00653 .04259 .03362 .05226 .01174 .03768 .01084 .02739 .00516 .00986

Order Clymeniida

.07519 .09789 .07040 .15919 .07853 .07986 .05960 .04834 .02938 .02461
.02366 .01073 .01171 .00773 .01410 .00979 .00953 .00704 .00435 .00439

Superfamily Gonioclymeniaceae
Family Acanthoclymeniidae
Genus Acanthoclymenia
species neopolitana

.06323 .07938 .09539 .23029 .10228 .11569 .08164 .07589 .05083 .04378
.04164 .01792 .02063 .01287 .02559 .01800 .01711 .01222 .00740 .00804

Superfamily Clymeniaceae
Family Clymeniidae
Genus Platyclymenia

.08715 .11640 .04540 .07808 .05478 .04403 .03755 .02078 .00793 .00543
.00568 .00353 .00278 .00258 .00260 .00158 .00195 .00185 .00130 .00073

Order Goniatitida

.03871 .04289 .02517 .02292 .03185 .05728 .05515 .06996 .05550 .04199
.03116 .02443 .03544 .02540 .02239 .02777 .01906 .01946 .02441 .02443

Superfamily Cheilocerataceae

.04573 .07560 .03598 .03916 .07009 .07606 .02257 .05186 .02674 .03236
.03139 .04706 .00692 .02240 .01880 .01704 .00968 .02347 .00524 .01548

Family Tornoceratidae

.05127 .06311 .04165 .05246 .05829 .10137 .00520 .06616 .01634 .01654
.01326 .03505 .00346 .02600 .01174 .01321 .00254 .01914 .00192 .01319

Family Cheiloceratidae

.04018 .08809 .03031 .02585 .08189 .05075 .03993 .03756 .03713 .04817
.04951 .04647 .01037 .01879 .02585 .02087 .01681 .02779 .00855 .01776

Superfamily Cyclolobaceae
Family Popanoceratidae
Subfamily Marathonitinae
Genus Peritrochia
species dieneri

.0528 .0431 .0084 .0153 .0088 .0022 .0036 .0218 .0022 .0308
.0087 .0262 .0179 .0248 .0006 .0317 .0037 .0084 .0391 .0619

Superfamily Agathicerataceae
 Family Agathiceratidae
 Genus Agathiceras
 species uralicum

.0259 .0415 .0331 .0055 .0079 .0773 .1007 .0666 .0507 .0289
 .0582 .0039 .0346 .0212 .0142 .0257 .0013 .0170 .0163 .0182

Superfamily Goniatitaceae

.04260 .03331 .03034 .03783 .04595 .09347 .06182 .12305 .11161 .05971
 .02411 .02986 .04467 .04217 .03708 .04229 .04404 .03594 .02970 .00815

Family Neiococeratidae

.0538 .0284 .0072 .0335 .0216 .0485 .0176 .2346 .1672 .0178
 .0073 .0365 .0553 .0844 .0405 .0835 .0295 .0384 .0241 .0230

Family Schitoceratidae
 Subfamily Schistoceratinae

.04980 .02590 .05452 .03170 .03655 .08070 .11608 .10283 .14580 .13065
 .04030 .02470 .05510 .03102 .04288 .03350 .06185 .05235 .03315 .02268

Superfamily Adrianitaceae
 Family Adrianitidae

.02690 .02095 .01803 .01680 .02650 .03738 .08705 .08650 .08623 .05819
 .03338 .02141 .07309 .01644 .04128 .02211 .03659 .01249 .03173 .00815

Subfamily Adrianitinae

.02429 .01189 .02035 .01090 .01630 .04715 .10529 .06959 .07425 .09067
 .01585 .03582 .05197 .01947 .00735 .02012 .03957 .02237 .02475 .01179

Subfamily Dunbaritinae
 Genus Emilites
 species incertus

.02950 .0300 .0157 .0227 .0367 .0276 .0688 .1034 .0982 .0257
 .0509 .0070 .0942 .0134 .0752 .0241 .0336 .0026 .0387 .0045

Order Cerititida
 Superfamily Otocerataceae
 Family Xenodiscidae

.02602 .04284 .06059 .04433 .08939 .18577 .10257 .08220 .06517 .02121
 .03966 .02877 .02061 .01668 .03424 .01734 .01884 .01566 .01574 .00834

APPENDIX E

APPENDIX E

Coefficients of Variation of the Harmonic Amplitudes for the Taxonomic Hierarchy.

Subclass Nautiloidea

Order Nautilida

Superfamily Nautilaceae

35.25	62.03	41.74	31.48	32.92	55.52	24.30	28.50	74.69	53.71
49.59	52.46	70.79	63.56	42.31	64.14	117.18	113.75	60.13	54.06

Family Hercoglossidae

66.39	62.25	63.63	46.00	52.77	38.55	42.74	106.42	28.88	37.22
140.10	114.41	77.92	78.52	84.99	106.18	65.59	55.83	95.71	64.20

Genus Deltoidonautilus

22.27	65.45	43.69	40.32	66.49	9.03	21.75	23.08	15.24	54.62
12.64	66.10	71.11	59.86	82.78	18.18	51.52	47.37	32.37	34.43

Genus Hercoglossa

60.98	70.60	56.34	26.91	68.27	23.13	26.22	14.42	26.69	60.85
65.74	67.88	81.06	115.52	54.56	124.36	64.91	51.27	22.98	88.12

Subclass Ammonoidea

43.80	51.81	46.52	64.81	32.87	49.46	27.98	10.46	40.42	28.49
46.48	52.26	36.67	31.49	32.10	20.56	19.08	25.19	54.79	70.46

Order Anarcestida

33.40	49.30	23.36	33.18	55.78	35.86	31.87	42.96	56.27	34.74
39.56	62.48	53.91	64.07	31.61	52.32	34.58	49.67	28.19	20.31

Superfamily Pharcicerataceae

Family Gephuroceratidae

51.04	83.29	62.64	11.39	71.01	76.08	26.57	52.11	36.58	58.54
51.48	79.27	112.68	66.87	64.14	69.10	73.17	15.26	26.90	44.64

Superfamily Anarcestaceae

46.76	38.57	86.99	67.72	45.46	60.65	23.09	48.80	10.99	31.95
22.95	27.16	27.58	35.72	42.53	45.08	37.61	39.02	40.49	42.70

Family Anarcestidae

69.25	47.99	102.55	34.32	12.83	44.52	36.52	81.09	39.99	36.58
41.12	11.18	42.14	16.32	19.19	8.46	19.97	7.68	.51	18.10

Family Agoniatitidae

25.62	6.35	2.91	11.46	61.97	2.34	22.77	7.68	47.48	10.02
69.63	7.09	45.17	11.24	40.36	12.36	31.30	17.91	36.08	22.10

Genus Agoniatites

29.30	12.87	7.26	12.86	80.24	3.36	19.42	9.10	5.83	25.68
23.50	12.27	25.74	18.22	16.90	33.41	33.33	30.34	28.28	28.60

Order Clymeniida

.26	15.12	58.65	44.34	35.33	58.08	59.26	70.33	62.62	76.96
70.77	54.82	79.26	28.26	89.96	90.86	88.61	79.54	81.09	81.23

Superfamily Clymeniaceae

Genus Platyclymenia

14.97	65.68	26.54	59.08	79.46	73.42	75.92	75.45	81.07	41.01
26.87	37.59	27.93	14.56	21.15	33.33	30.77	2.70	7.69	58.62

Order Goniatiitida

27.23	42.49	41.24	58.05	74.23	57.86	67.14	48.47	71.10	33.10
51.56	49.46	64.65	34.70	67.06	31.30	92.98	49.54	49.51	78.19

Superfamily Adrianitaceae

Family Adrianitidae

9.69	43.23	12.90	35.12	38.49	26.15	20.96	19.54	13.89	55.83
52.51	67.30	28.89	18.47	82.19	9.00	8.16	79.18	21.99	44.75

Subfamily Adrianitinae

86.54	53.13	72.48	44.04	68.71	79.64	77.04	58.80	11.38	31.69
16.09	99.16	76.33	8.91	64.63	50.29	87.29	40.53	88.69	10.90

Superfamily Goniatiitiaceae

30.77	26.32	63.71	19.66	53.61	45.89	66.04	68.30	57.41	84.46
55.91	16.50	33.35	73.39	17.76	72.57	30.44	40.38	13.45	34.04

Family Goniatiitidae

74.80	48.26	92.49	78.38	55.02	7.02	95.17	73.65	46.64	62.20
99.39	48.40	29.69	90.53	2.04	69.11	12.30	30.54	23.84	31.41

Subfamily Goniatiitinae

5.77	1.18	29.10	9.25	78.52	22.02	.90	70.70	50.65	85.54
55.85	5.76	37.47	7.65	.32	74.25	2.24	13.77	26.32	34.66

Family Schistoceratidae

5.77	1.81	2.10	9.25	78.52	22.02	.90	70.70	50.65	85.54
55.85	5.76	37.47	7.65	.32	74.25	2.24	13.77	26.32	24.66

Superfamily Cheilocerataceae

12.13	16.52	15.76	33.98	16.84	33.28	76.96	27.57	38.88	48.88
57.75	14.01	49.96	16.10	37.54	22.48	73.75	18.43	63.32	14.77

Family Cheiloceratinae

40.96	19.57	98.40	83.52	70.48	41.74	31.41	120.78	66.21	61.19
76.98	104.62	53.29	89.00	78.08	58.62	59.57	92.37	61.37	90.92

Subfamily Cheiloceratidae

90.60	41.58	101.77	28.91	31.69	48.42	70.84	13.02	45.50	77.44
72.60	112.49	13.82	69.16	43.12	6.28	60.64	54.81	75.82	57.24

Family Tornoceratidae

78.15	13.25	29.17	56.82	42.13	32.12	63.46	42.03	10.19	7.80
17.27	29.53	95.66	51.92	39.95	57.23	35.83	55.06	61.88	76.12

Order Cerititida

Superfamily Otocerataceae

Family Xenodiscidae

47.48	39.61	84.48	48.15	65.50	16.03	20.41	73.44	57.32	74.24
25.73	46.23	50.71	32.95	50.14	30.55	30.32	58.83	29.11	45.02

Genus Paraceltites

30.91	18.66	30.53	52.95	33.29	34.66	54.36	23.80	69.40	36.40
31.53	12.70	47.35	67.24	37.57	28.46	32.50	40.55	69.59	41.36

APPENDIX F


```

PROGRAM FILTER (INPUT, OUTPUT, TAPES)
DIMENSION IBUF (2049), NAME (3, 3), X (1001), LETTER (3)
COMMON Y (1001), AMP (20, 3), FAZE (20, 3)
DATA NAME (1, 3), NAME (2, 3), NAME (3, 3) / 10H      RES,
* 10H IDUAL SIGN, 10HAL
DATA LETTER / 1HA, 1HB, 1HC /
CALL PLOTS (IBUF, 2049, 5)
CALL PLOT (1.0, 9.0, -3)
DO 50 N=1, 2
READ (5, 1) (NAME (I, N), I=1, 3)
READ (5, 2) (AMP (I, N), I=1, 20)
READ (5, 2) (FAZE (I, N), I=1, 20)
50 CONTINUE
X (1) = 0.0
DO 75 I=2, 1001
75 X (I) = X (I-1) + 0.00575
C----- COMPUTE RESIDUAL CURVE
DO 100 I=1, 20
AMP (I, 3) = ABS (AMP (I, 1) - AMP (I, 2))
FAZE (I, 3) = FAZE (I, 1)
IF (AMP (I, 2) .GT. AMP (I, 1)) FAZE (I, 3) = FAZE (I, 2)
100 CONTINUE
DO 200 N=1, 3
CALL LODER (N)
CALL SYMBOL (0.05, -1.5, 0.2, LETTER (N), 0, 1)
CALL ARROW (X (1), Y (1))
CALL PLOT (X (1), Y (1), 3)
DO 150 I=2, 1001
150 CALL PLOT (X (I), Y (I), 2)
CALL ARROW (X (1001), Y (1001))
CALL ARROW (X (501), Y (501))
CALL SYMBOL (0.75, -1.5, 0.15, NAME (1, N), 0, 30)
CALL PLOT (0.0, -3.0, -3)
200 CONTINUE
PRINT 3, (NAME (I, 3), I=1, 3)
PRINT 4, (AMP (I, 3), I=1, 20)
PRINT 4, (FAZE (I, 3), I=1, 20)
DO 300 I=1, 100
300 X (I) = X (I + 10) * 1.092728
Y (I) = Y (I + 10) * 1.092728
CALL FTEST (X)
1
4
FORMAT (3A10)
FORMAT (10F7.4/10F7.4)
FORMAT (1H0, 3A10)
FORMAT (1X, 10F7.4/1X, 10F7.4)
CALL PLOT (0.0, 0.0, 999)
END

```

```

100
110
120
130
140
150
160
170
180
190
200
210
220
230
240
250
260
270
280
290
300
310
320
330
340
350
360
370
380
390
400
410
420
430
450
460
470
480
490
500
510
520
530
540
550
560

```

	SUBROUTINE LODER (N)	570
	COMMON Y(1001),AMP(20,3),FAZE(20,3)	580
	Y(I)=0.0	590
10	DO 10 K=1,20	600
	Y(I)=Y(I)+AMP(K,N)*SIN(FAZE(K,N))	610
C-----	MULTIPLY BY THE SCALE FACTOR	620
	Y(I)=Y(I)*0.915141	630
	X=0.0	640
	DO 20 I=2,1001	650
	X=X+0.0528318	660
	Y(I)=0.0	670
	DO 30 K=1,20	680
30	Y(I)=Y(I)+AMP(K,N)*SIN(K*X+FAZE(K,N))	690
	CONTINUE	700
20	Y(I)=Y(I)*0.915141	710
	CONTINUE	720
	END	730

	SUBROUTINE_ARROW(X,Y)	740
	ASS = Y-0.75	750
	POINT = Y+0.75	760
	CALL PLOT (X,ASS,3)	770
	CALL PLOT (X,POINT,2)	780
	R=X+0.125	790
	RNOT=X-0.125	800
	DROP=POINT-0.125	810
	CALL PLOT (R,DROP,2)	820
	CALL PLOT (RNOT,DROP,3)	830
	CALL PLOT (X,POINT,2)	840
	END	850

```

SUBROUTINE FTEST(X)
DIMENSION YNEW(101),F(20),RMS(20),X(101)
COMMON Y(1001),AMP(20,3),FAZE(20,3)
INTEGER DFD(20)
C----- INITIALIZE SSE2
SSE2=0.0
DO 10 J=1,101
YNEW(J)=0.0
C----- COMPUTE SUM OF SQUARED ERROR OF A0 (=0.0) FROM ORIGINAL DATA
SSE2=SSE2+Y(J)*Y(J)
10 CONTINUE
DO 20 I=1,20
C----- COMPUTE NEW APPROXIMATION WITH THE ADDITION OF HARMONIC I
DO 20 J=1,101
YNEW(J)=YNEW(J)+AMP(I,3)*SIN(I*X(J)+FAZE(I,3))
20 CONTINUE
C----- MAKE OLD #MODEL2# INTO NEW #MODEL1#
SSE1=SSE2
C----- INITIALIZE SSE2
SSE2=0.0
C----- COMPUTE DEGREES OF FREEDOM FOR THE DENOMINATOR
DFD(I)=101-I-1
C
C----- DEGREES OF FREEDOM FOR THE NUMERATOR ALWAYS = ONE
C
C----- COMPUTE SUM OF SQUARED ERROR OF NEW APPROXIMATION
FROM ORIGINAL DATA
DO 30 J=1,101
SSE2=SSE2+(Y(J)-YNEW(J))**2
30 CONTINUE
C----- COMPUTE ROOT MEAN SQUARE ERROR
RMS(I)=SQRT(SSE2/100.)
C----- COMPUTE F-STATISTIC
F(I)=(SSE1-SSE2)/(SSE2/DFD(I))
50 CONTINUE
PRINT 1,RMS
PRINT 2,F
PRINT 3,DFD
1
3
FORMAT(0)
FORMAT(*)
FORMAT(*)
FORMAT(*)
END

```

```

860
870
880
890
900
910
920
930
940
950
960
970
980
990
1000
1010
1020
1030
1040
1050
1060
1070
1080
1090
1100
1110
1120
1130
1140
1150
1160
1170
1180
1190
1200
1210
1220
1230
1240
1250
1260
1270
1280

```